



# Application of biochar in advanced oxidation processes: supportive, adsorptive, and catalytic role

Faheem<sup>1</sup> · Jiangkun Du<sup>1</sup> · Sang Hoon Kim<sup>2</sup> · Muhammad Azher Hassan<sup>3</sup> · Sana Irshad<sup>1</sup> · Jianguo Bao<sup>1</sup>

Received: 9 August 2019 / Accepted: 1 January 2020  
© Springer-Verlag GmbH Germany, part of Springer Nature 2020

## Abstract

The advanced oxidation processes (AOPs), especially sulphate radical ( $\text{SO}_4^{\bullet-}$ )-based AOPs (SR-AOPs), have been considered more effective, selective, and prominent technologies for the removal of highly toxic emerging contaminants (ECs) due to wide operational pH range and relatively higher oxidation potential (2.5–3.1 V). Recently, biochar (BC)-based composite materials have been introduced in AOPs due to the dual benefits of adsorption and catalytic degradation, but the scientific review of BC-based catalysts for the generation of reactive oxygen species (ROSs) through radical- and non-radical-oriented routes for EC removal was rarely reported. The chemical treatments, such as acid/base treatment, chemical oxidation, surfactant incorporation, and coating and impregnation of minerals, were applied to make BC suitable as supporting materials (SMs) for the loading of Fenton catalysts to boost up peroxymonosulphate/persulphate/ $\text{H}_2\text{O}_2$  activation to get ROSs including  $\bullet\text{OH}$ ,  $\text{SO}_4^{\bullet-}$ ,  $^1\text{O}_2$ , and  $\text{O}_2^{\bullet-}$  for targeted pollutant degradation. In this review, all the possible merits of BC-based catalysts including supportive, adsorptive, and catalytic role are summarised along with the possible route for the development prospects of BC properties. The limitations of SR-AOPs especially on production of non-desired oxyanions, as well as disinfection intermediates and their potential solutions, have been identified. Lastly, the knowledge gap and future-oriented research needs are highlighted.

**Keywords** Biochar · Advanced oxidation processes · Heterogeneous catalyst · Wastewater · Catalytic degradation

## List of abbreviations

|      |                              |
|------|------------------------------|
| AC   | Activated carbon             |
| AOPs | Advanced oxidation processes |
| BC   | Biochar                      |
| CNTs | Carbon nanotubes             |
| CPC  | Cetylpyridinium chloride     |
| DOM  | Dissolved organic matter     |

|                         |                                  |
|-------------------------|----------------------------------|
| ECs                     | Emerging contaminants            |
| EDCs                    | Endocrine-disrupting chemicals   |
| FGs                     | Functional groups                |
| HTT                     | Heat treatment temperature       |
| $\text{O}_2^{\bullet-}$ | Superoxide radicals              |
| SMZ                     | Sulfamethoxazole                 |
| RhB                     | Rhodamine B                      |
| SD                      | Sulfadiazine                     |
| PFRs                    | Persistent free radicals         |
| MOFs                    | Metal organic frameworks         |
| OFGs                    | Oxygen functional groups         |
| PCP                     | Pentachlorophenol                |
| PMS                     | Peroxymonosulphate               |
| PDS                     | Peroxydisulphate                 |
| PS                      | Persulphate                      |
| HDBPs                   | Harmful disinfection by-products |
| ROSs                    | Reactive oxygen species          |
| SMs                     | Supporting materials             |
| SR-AOPs                 | Sulphate radical-based AOPs      |
| TC                      | Tetracycline                     |
| IBF                     | Ibuprofen                        |
| NBCs                    | N-doped biochars                 |

Responsible editor: Vitor Pais Vilar

✉ Jiangkun Du  
dujk@cug.edu.cn

✉ Jianguo Bao  
bjianguo@cug.edu.cn

<sup>1</sup> School of Environmental Studies, China University of Geosciences, 430074 Wuhan, People's Republic of China

<sup>2</sup> Materials Architecturing Research Center, Korea Institute of Science and Technology, Seoul 136-791, Korea

<sup>3</sup> Tianjin Key Laboratory of Indoor Air Environmental Quality Control, School of Environmental Science and Engineering, Tianjin University, Tianjin 300072, China

## Introduction

To cope with rapid population expansion, an intense increase in agricultural and industrial activities causes huge solid waste generation and wastewater production. The direct discharge of wastewater from these industries into receiving water bodies is considered the main source of spreading contamination of highly toxic emerging contaminants (ECs) and refractory contaminants including endocrine-disrupting chemicals (EDCs), agrochemicals, pharmaceuticals, and organic dyes (Boix et al. 2016). Traditional wastewater treatment technologies such as biodegradation through microorganism and physical and chemical processes including adsorption, filtration, and flocculation could be applied to treat kinds of anthropogenically originated polluted water. However, limitations of these conventional treatment methods could be reflected by their high costs for posttreatment of generated secondary pollutants due to non-destructive or just phase transformation of contaminants instead of complete mineralisation in order to get non-toxic products such as  $\text{CO}_2$ ,  $\text{H}_2\text{O}$ , and inorganic salts (Chi et al. 2013; Dantas et al. 2006; Georgi and Kopinke 2005; Prieto-Rodríguez et al. 2013; Snyder et al. 2007). Consequently, these methods are not desirable for the destruction of ECs which are less biodegradable and recalcitrant in wastewater.

Recently, advanced oxidation processes (AOPs) have received increasing attention both from academic and industrial point of view because of the strong destructive capability for ECs. During AOPs, highly strong oxidising species ( $\cdot\text{OH}$ ,  $\text{SO}_4^{\cdot-}$ ,  $\text{O}_2^{\cdot-}$ ,  $^1\text{O}_2$ ) are produced for the destruction of recalcitrant organic pollutants. The advantages of high redox potentials for both sulphate radicals ( $\text{SO}_4^{\cdot-}$ ,  $E^0 = 2.5\text{--}3.1\text{ V}$ ) and hydroxyl radicals ( $\cdot\text{OH}$ ,  $E^0 = 1.9\text{--}2.7\text{ V}$ ), selectivity for a wide range of organic contaminants, and relatively low cost, make AOPs promising for the treatment of recalcitrant organic pollutants present in wastewater. In case of decomposition of organic pollutants by interacting with strong oxidising species in AOPs, innocuous or less toxic compounds form and complete mineralisation results in non-toxic products such as  $\text{CO}_2$ ,  $\text{H}_2\text{O}$ , and inorganic salts. For the last few decades, catalysts containing redox metals have received increasing attention for the generation of highly oxidising species, such as  $\cdot\text{OH}$  and  $\text{SO}_4^{\cdot-}$  radicals, through peroxymonosulphate (PMS), persulphate (PS), or hydrogen peroxide ( $\text{H}_2\text{O}_2$ ) activation, respectively. Figure 1 provides the classification of AOPs based on the presence of energy supply from an external source. Metal-mediated activation processes are technoeconomically more feasible than thermal-, UV-, ultrasound-, light-, and base-activated methods which require extra chemical and energy to facilitate activation as shown in Fig. 1 (Deng et al. 2014; Gao et al. 2016; Wang et al. 2016b). In addition, due to the short life cycle of  $\text{SO}_4^{\cdot-}$  and  $\cdot\text{OH}$  (about 4 s and 20 ns, respectively), their interaction with aqueous substrates is temporally limited and may result in

unsatisfactory or less oxidising efficiency towards organic pollutants (Yang et al. 2011). Therefore, enhancing the pollutants transfer from aqueous phase onto catalyst surface is an effective pathway to facilitate their oxidation during heterogeneous AOPs because the radical generation in most cases occurs on catalyst surface (Lee et al. 2013). For example, use of activated carbon (AC) as supporting materials (SMs) for the loading of  $\text{RuO}_2$  to obtain  $\text{RuO}_2/\text{AC}$  composite that exhibited higher phenol degradation in peroxymonosulphate activation system due to higher adsorption capacity of  $\text{RuO}_2/\text{AC}$  for phenol, which had more chances for interacting with oxidising radicals (Muhammad et al. 2012). Studies using bare  $\text{Co}_3\text{O}_4$  nanoparticles and metal organic framework (MOFs)-based composite  $\text{Co}_3\text{O}_4@\text{MOF}$  with yolk-shell configuration also confirmed the improved degradation of organic pollutants due to the accumulation of pollutants on catalyst surface through adsorption during the initial stage and followed by radical-induced degradation during the later stage (Zeng et al. 2014). However, it should require a lot of budget in terms of chemicals and energy to artificially synthesise such multifunctional composite material by combining active components, heterogeneous support, and other building blocks together. It is recommended to reduce the cost as much as possible by using highly efficient synthetic routes and with less chemical consumption in order to launch an advanced technology from benchtop experiments to commercial levels.

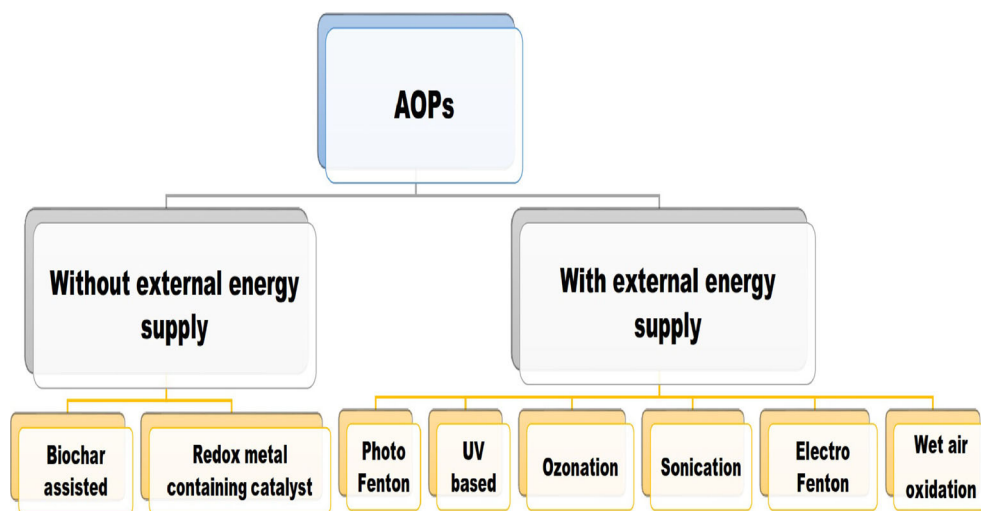
To tackle this issue, the use of low-cost SMs such as BCs obtained after pyrolysis of abundantly available biomass is one of the best choices to be an alternative for commercially available SMs, e.g. clays and zeolites. BC with mesoporous structure is considered high surface area and abundant oxygen functional groups (OFGs). Inspired by these unique properties, BC has been frequently applied as a fascinating support media in heterogeneous AOPs. This review aims to highlight the most recent advances of BC-based heterogeneous catalysts for the degradation of recalcitrant organic pollutants. The progress of BC production methodologies and different modification techniques were reviewed, especially focused on chemical modifications for tuning the BC properties. The main obstacles of sulphate radical-based AOPs (SR-AOPs), such as the additional production of unwanted species like oxyanions and harmful disinfection by-products (HDBPs) of carcinogenic nature, proper handling, and further treatment of sulphate as well as excessively available PMS, are also discussed in detail.

## Biochar with intrinsic adsorption peculiarity

### Tuning biochar surface properties for oxidation processes

Biochar is typically derived from a different variety of agriculture waste biomass such as dairy manure, agricultural

**Fig. 1** Classification of advance oxidation process (AOP) based on energy supply and without energy supply from an external source



residue, and food waste through pyrolysis or charring process in which biomasses are subjected to thermochemical conversion under an oxygen-limited condition at a temperature ranging from 300 to 800 °C (Kim et al. 2017; Manyà et al. 2018). Figure 2 gives a quick review of the different approaches applied for BC production and treatment routes for BC surface modification. The BC obtained by direct pyrolysis of biomass gives poor physiochemical properties such as surface OFGs, surface area, pore volume, and pore width. However, the available functional groups (FGs) on BC, surfaces such as carboxyl (–COOH), hydroxyl (–OH), and carbonyl (C=O), are quite important for the accumulation of contaminants from water and wastewater. The hydrophilic (polarity index) or hydrophobic property (aromaticity) of BC depends upon the type and nature of existing FGs on the surface. There are different

techniques available to boost up the abundance of FGs, such as steam activation, impregnation method, and chemical and heat treatment as shown in Fig. 2 (Shen et al. 2008). These treatment techniques can increase surface area and OFGs and improve porous structures, which are directly associated with the sorption of organic and inorganic contaminants in single-solute or binary-solute aqueous solutions. These properties significantly influence the performance of BC-based catalysts during their various applications. Therefore, it is extremely essential to choose the best protocol or scheme for BC-based catalyst preparation so as to obtain dual properties of adsorption in the first stage and catalytic ability in the later stage, which should accelerate the efficient utilisation of reactive oxygen species (ROSs) for contaminant degradation on the BC-based catalyst surface.

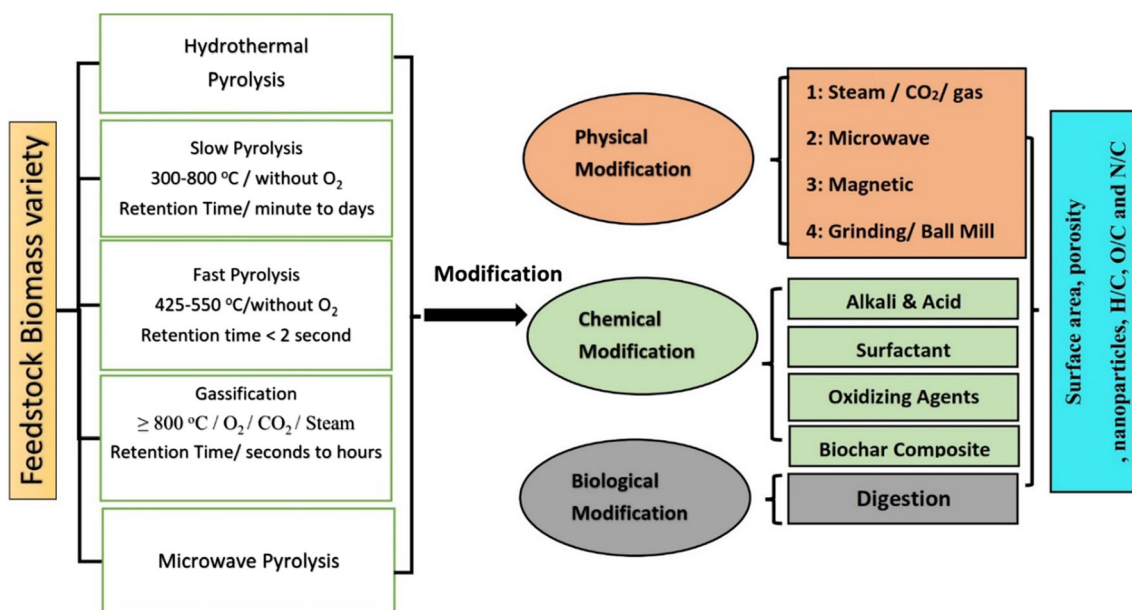


**Fig. 2** Quick overview of the approaches for BC production and treatment technologies for BC modification purpose

## Modified biochar with enhanced adsorption for oxidation processes

Different chemical reagents (e.g.  $\text{HNO}_3$ ,  $\text{H}_2\text{SO}_4$ ,  $\text{HCl}$ ,  $\text{H}_3\text{PO}_4$ ,  $\text{NaOH}$ ,  $\text{KOH}$ , oxalic acid,  $\text{H}_2\text{O}_2$ , potassium permanganate, ozone, and ammonium persulphate) have been extensively applied for the production of desired chemical changes or FGs onto BC matrix (Tang et al. 2018). Despite additional cost for the different types of BC treatment, the end beneficial BC properties after the treatment make them feasible options.

Among these treatments, acid washing is an effective method to enhance surface acidity and porous structure of BC and at the same time remove available metal impurities. Presence of mineral (ash) components in the form of carbonates, phosphates, or oxides can pose both positive and negative effects on the supportive removal of organic contaminants (Xu et al. 2017). For example, in case of BC oxidation through  $\text{HNO}_3$  treatment, the decrease in the total surface area was observed because of the breakage of pore wall and expansion of micropores into meso- or macro-pores during the  $\text{HNO}_3$  erosion (Yakout 2015). Similarly, a decrease trend in BC porosity by 10–40% was noticed when  $\text{H}_2\text{SO}_4$  treatment was applied (Liu et al. 2012). However, wheat straw-derived BC modified with different concentrations of  $\text{HCl}$  (1.0 mol/L and 6.0 mol/L) developed more heterogeneous porous structure compared with untreated samples (Li et al. 2014b). In addition, treatment using phosphoric acid ( $\text{H}_3\text{PO}_4$ ) is considered to be an environmentally friendly approach than using other available corrosive and hazardous chemicals, such as  $\text{ZnCl}_2$  (Guan et al. 2015).  $\text{H}_3\text{PO}_4$  treatment triggered more porosity development due to the formation of phosphate and polyphosphate which act as a kind of cross bridge to minimise shrinkage or contraction during the decomposition of lignocellulosic, aromatic, and aliphatic components (Guan et al. 2015). Typically, carboxylic and ketonic groups, amine groups, and other oxygen-containing moieties are expected to increase on BC surfaces, and more polar and hydrophilic natures should form after acid modification to enhance adsorptive removal of organic contaminants and metal ions.

In contrast to acidic modification, treatment with alkaline improves not only chemical but also physical properties of BC due to the dissolution of available ash and condensed organic matter, such as celluloses and lignin, resulting in the higher surface area than acid-modified BC (Feng and Zhu 2017). The alkali treatment brings an increase in aromaticity, which makes BC more hydrophobic in nature. For example, the  $\text{NaOH}$ -activated pine BC possessed a relatively large surface area of 1151 and 1360  $\text{m}^2 \text{g}^{-1}$  under oxygen ( $\text{NaOH-O-BC}$ ) and nitrogen ( $\text{NaOH-N-BC}$ ) environment, respectively. Moreover, the  $\text{NaOH-N-BC}$  demonstrated higher adsorption capacity for atrazine, sulfamethoxazole, chloramphenicol, bisphenol-A, and carbamazepine due to more surface area and pore volume (Jung et al. 2013). Sorption trend with the

$\pi$ - $\pi$  interaction between sorbent and sorbate due to  $\pi$ -orbital energy at an atomic level declared as chemisorption. Take  $\text{KOH}$  treatment as an example, the formation of  $\text{K}_2\text{O}$ ,  $\text{K}_2\text{CO}_3$  through metallic K intercalation with the lattice of carbon matrix or crystallite layer during activation at high temperatures ( $> 775^\circ\text{C}$ ) resulted in expansion of carbon lattice, which facilitated widening of existing pores and new pore formation. It was observed that BC surface FGs almost remained constant after  $\text{KOH}$  activation, and the enhancement of adsorptive removal of  $\text{Cd}^{2+}$  and  $\text{Cu}^{2+}$  cations was attributed to the increase in surface area and high amounts of OFGs (Regmi et al. 2012). Moreover, the alkaline chemicals with  $\text{OH}^-$  ion or  $-\text{NH}_2$  group would coordinate with the BC surface FGs, thus further accelerate the sorption ability for organic contaminants and negatively charged pollutants in wastewater. For example, acrylonitrile grafting into lignin of BC matrix remarkably enhance the removal of  $\text{Cd}^{2+}$  from water by ion exchange and adsorption-complexation mechanism (Luo et al. 2018). Phenol removal was increased sharply when urea modification was applied to AC which caused the formation of N-associated FGs (pyridinic groups) and an increase of surface basicity (Yang et al. 2014). In addition, the removal of organic pollutants could be accelerated through  $\pi$ - $\pi$  electron donor and acceptor mechanism between BC graphitic structure and aromatic rings of targeted pollutants. Liu et al. also confirmed the higher removal of tetracycline (TC) in the case of  $\text{KOH}$ -modified BC (58.52  $\text{mg g}^{-1}$ ) than most studies (4.5–54  $\text{mg g}^{-1}$ ) (Liu et al. 2012). Similarly,  $\text{NaOH}$ -modified BC applied for chloramphenicol removal exhibited significantly higher removal efficiency as compared with untreated BC (Fan et al. 2010).

Except for severe acidic and basic modifications (Azargohar and Dalai 2008; Uchimiya et al. 2010; Yang and Jiang 2014), the strong oxidant  $\text{H}_2\text{O}_2$  can also be utilised to produce the desired surface chemistry of BC materials. The  $\text{H}_2\text{O}_2$  modification is recognised as a relatively cost-efficient and environmentally friendly method. After being employed, few residual  $\text{H}_2\text{O}_2$  remained on BC surface because most of  $\text{H}_2\text{O}_2$  decomposed into clean products of  $\text{O}_2$  and  $\text{H}_2\text{O}$  in the end. The literature study confirmed that the treatment of  $\text{H}_2\text{O}_2$  and other oxidising agents would increase OFGs on BC surface (Yakout 2015). As indicated by FTIR spectra, C=O, alcoholic, quinone or a conjugated quinone, lactonic, and carboxyl-carbonate FGs were found on  $\text{H}_2\text{O}_2$ -treated BC samples. BC modification with a variety of oxidising agents ( $\text{H}_2\text{O}_2$ ,  $\text{KMnO}_4$ ,  $\text{KOH}$ ,  $\text{HNO}_3$ , and  $\text{H}_2\text{SO}_4$ ) exhibited higher adsorption capacities for phenol and methylene blue from aqueous solutions. The higher adsorption of phenol and methylene blue was due to change in acidity/alkalinity and hydrophilicity of modified BC after treatment with a different oxidising agent as compared with parent BC samples. Moreover, patchouli BC  $\text{Cr}_2\text{O}_3$  composite has been synthesised successfully for the remediation of paracetamol-contaminated wastewater

through adsorption. It was revealed that the type of oxidising agents ( $\text{H}_2\text{SO}_4\text{-HNO}_3$ ,  $\text{H}_3\text{PO}_4\text{-HNO}_3$ ,  $\text{H}_2\text{O}_2\text{-HNO}_3$ ) affected the contents of  $\text{Cr}_2\text{O}_3$  in the composite, surface FGs of BC before impregnation, and paracetamol adsorption capacity (Setianingsih et al. 2018). Chen et al. confirmed the effectiveness of granular fir-based activated carbon (GFAC) modified by  $\text{H}_2\text{O}_2$  for the removal of a variety of pollutants (Chen et al. 2014). For set-optimised boundary conditions, caramel decolourisation, methylene blue adsorption performance, phenol adsorption removal, and an iodine number of the modified GFAC increased by 500.0%, 59.7%, 32.5%, and 15.1%, respectively. In another study, partial oxygenation of BC was introduced through  $\text{H}_2\text{O}_2$  treatment, resulting in enhancement of BC cation exchange capacity (Huff and Lee 2016). The increment of the available OFGs on hydrochar (carbon-rich material obtained through biomass by hydrothermal conversion) surface was also observed after  $\text{H}_2\text{O}_2$  treatment, which enhanced its sorption affinity towards aqueous ammonium and heavy metals (Wang et al. 2015; Wang et al. 2016a). Lead adsorption ability was tested for available commercial AC, pristine hydrochar, and  $\text{H}_2\text{O}_2$ -oxidised hydrochar. The  $\text{H}_2\text{O}_2$ -oxidised hydrochar exhibited higher lead removal with an adsorptive capability of about  $22.82 \text{ mg g}^{-1}$ , which was comparable to with commercially available AC applied during experiments and was 20 times higher than that of untreated hydrochar adsorption efficiency (Xue et al. 2012). Besides the adsorptive role of BC, Fang et al. applied BC as the catalyst to activate  $\text{H}_2\text{O}_2$  to generate  $\cdot\text{OH}$  radicals for the degradation of 2-chlorobiphenyl (Fang et al. 2014). The application of low-cost and environmental friendly  $\text{H}_2\text{O}_2$  as compared with other available oxidants is beneficial especially when the modified BC is employed for purification of drinking water and soil amendment, where the entry of any other interfering matter or elements is undesirable in order to avoid any side reactions (Huff and Lee 2016).

Surfactants have also been utilised to modify the surface properties of a variety of solid materials including BC, bentonite, and zeolite. Based on the nature of the hydrophilic group, surfactants can be classified into anionic, cationic, non-ionic, and Gemini types (Paria 2008). Due to the negatively charged surface of BC, the cationic surfactant can easily interact with BC through electrostatic attraction or by exchange with available cations, such as  $\text{Na}^+$ ,  $\text{K}^+$ , and  $\text{Mg}^{2+}$ , in BC skeleton, and thus results in surfactant-biochar complex (Erdinc et al. 2010). A cationic surfactant tetradecyltrimethyl ammonium bromide (TTAB) was applied for switchgrass BC (SB) modification to get a novel SB-TTAB adsorbent in order to increase adsorption ability for reactive red 195 A dye (RR-195A). The efficient removal of the RR-195A dye was achieved with excellent recovery values in the range 90–100% when SB-TTAB adsorbent was employed in tap water, raw water, wastewater, and seawater (Mahmoud et al. 2016). Moreover, Saleh et al. studied the sorption of cationic

surfactant, cetylpyridinium chloride (CPC), onto granular charcoal at different concentration levels (Saleh 2006). The combination of CPC on charcoal was mainly due to ion exchange at low CPC concentrations, and the surface adsorbed water was replaced by CPC molecules. With increasing aqueous CPC concentration, a chain-chain layer was expected to form to stabilise surfactant adsorption. As CPC concentration further increased, CPC micelles tended to be the dominant form but not adsorbed onto charcoal. Similarly, Han et al. studied the sorption of pentachlorophenol (PCP) by BC and AC in the presence of a cationic surfactant (Han et al. 2013). Cationic surfactant cetyltrimethyl ammonium bromide (CTAB) was first mixed with PCP solution, and then, the BC was added and modified with CTAB through ion-exchange mechanism along with enhanced sorption of PCP at the same time on the freshly formed BC-CTAB complex. In a word, BC can be modified by applying effective surfactant agent to enhance the removal efficiency of targeted anionic pollutants.

Carbon nanotube (CNTs)-modified hickory BC (HC-SDBC-CNT) and bagasse BC (BC-SDBC-CNT) were produced in the presence of anionic surfactant sodium dodecylbenzene sulfonate (SDBS) through dip-coating method followed by slow pyrolysis of coated biomass. The synthesised composite materials could effectively remove both sulfapyridine (SPL) and lead (Pb) in single-solute as well as binary-solute solutions due to the heterogeneity of surface functionalities or available active sites. It was noticed that maximum removal of 86% for SPL and 71% for Pb was achieved by using HC-SDBC-CNT (Inyang et al. 2015).

Sorption of nonionic surfactant to the charcoal surface is governed by physical sorption as depicted by low free energy changes during the sorption (Santhanalakshmi and Balaji 1996). The TX-100 loading of about  $300 \text{ mg g}^{-1}$  was noticed on charcoal (Hamid et al. 2014). Conversely, as a result of electrostatic repulsion forces, both micellar and monomolecular anionic surfactants were not able to adsorb onto BC surface. For example, minimal or slight sorption was observed for anionic surfactant by charcoal (Fujita et al. 1991). However, charcoal after activation could exhibit significant sorption ability for anionic surfactants such as sodium dodecyl (Erdinc et al. 2010).

## Biochar applied as the catalyst support

The loading or impregnation of metal catalysts on SMs is a potential strategy to resolve the problems encountered during homogeneous Fenton reactions, such as highly acidic reaction conditions, excessive release of transition metals in the effluent, metal sludge disposal, and slow reaction kinetics. Commercially, there are many SMs available which have been utilised for heterogeneous Fenton catalysts, such as AC

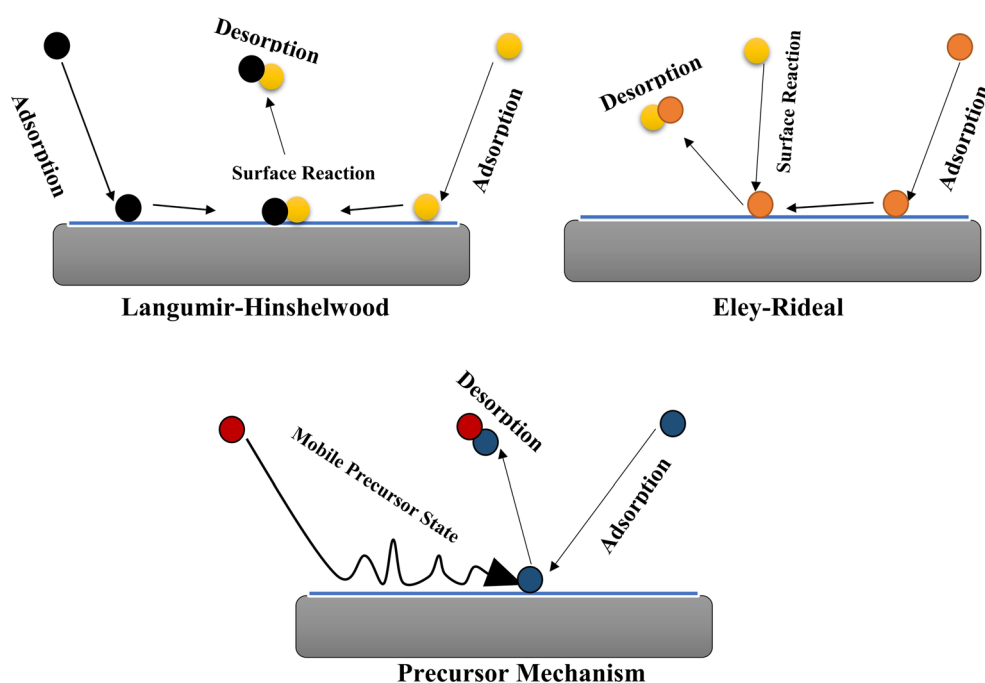
(Dantas et al. 2006; Georgi and Kopinke 2005; Lan et al. 2015; Zazo et al. 2006), BC (Deng et al. 2018), alumina (Bautista et al. 2010; Kunde and Yadav 2015), and zeolite. Thus, researchers have paid much attention to the development of supporting medium for the synthesis of highly efficient heterogeneous Fenton catalysts with both adsorption and oxidation ability (Song et al. 2015). In case of catalyst supports, the reaction could occur either on the surface of SMs or on the catalyst surface (Fig. 3). Basically, surface reactions can be described by one of these three mechanisms (Masel 1996): (i) the Langmuir-Hinshelwood mechanism, two molecules X and Y both adsorb first on the surface. While adsorbed on the solid surface, X and Y make a bond or meet, and then, new molecule X-Y finally desorbs (Hazime et al. 2014; Masel 1996). (ii) The Eley-Rideal mechanism, X adsorbs on the surface first, and then, second molecule Y interacts with X on the surface while not being desorbed from the surface, so they react and bind together as a new molecule X-Y and then desorbs (Hutchings 2015; Masel 1996). (iii) Precursor mechanism, one of the two molecules, X, is adsorbed on the surface. The second molecule, Y, collides with the surface to attain a mobile precursor state. The molecule Y then collides with molecule X on the surface. They react and bind, and newly formed molecule desorbs at last (Masel 1996; Wang et al. 2014). The synergistic effect between adsorption and oxidation abilities of heterogeneous Fenton catalysts favours the maximum utilisation of  $\text{H}_2\text{O}_2$ /PS/PMS, which are the main precursor of ROSs like  $\cdot\text{OH}$ ,  $\text{SO}_4^{\cdot-}$ , singlet oxygen ( $^1\text{O}_2$ ), and superoxide radicals ( $\text{O}_2^{\cdot-}$ ).

Biochar is one of the most promising supporting media for heterogeneous catalysis. The attractive features of BC, such as higher surface area as well as OFGs and abundant aromatic moieties, assist in creating synergistic adsorption and degradation of pollutants through  $\text{OH}$ ,  $\text{SO}_4^{\cdot-}$ ,  $^1\text{O}_2$ , and  $\text{O}_2^{\cdot-}$  oxidation. Moreover, the mesoporous structure of BC facilitates the good distribution of immobilised metallic nanoparticles and thus suppresses the agglomeration or aggregation of nanoparticles due to intraparticle interaction. The attachment or immobilisation of metal catalysts (Cu, Mn, Fe, and Co) onto adsorbent pores results in no or less metal release into treated effluents (Jafari et al. 2017; Zhang et al. 2016). Therefore, this strategy controls the leaching problem to avoid secondary pollution.

### Coating functional nanoparticles onto biochar

In order to increase the sorption capacity of BC for organic and inorganic pollutant removal, the functionalisation of BC with nanoparticles through dip-coating procedure has been recently used. A quick review of various proposed mechanisms for pollutant removal by modified BC is summarised in Fig. 4. The sorption of a variety of pollutants is achieved due to the involvement of different factors including (1) electrostatic interactions, (2) pore-filling, (3) adsorption followed by reduction, (4) hydrophobic, (5)  $\pi$ - $\pi$  and cation- $\pi$  interactions, (6) electron and hole pair interaction pathway, and (7) hydrogen bonding. For instance, 5 times more removal of anionic dye, named as directly frozen yellow (DFY), could be achieved through MgO-coated biochar (MC) sorption as

**Fig. 3** Surface reactions described by possible three mechanisms



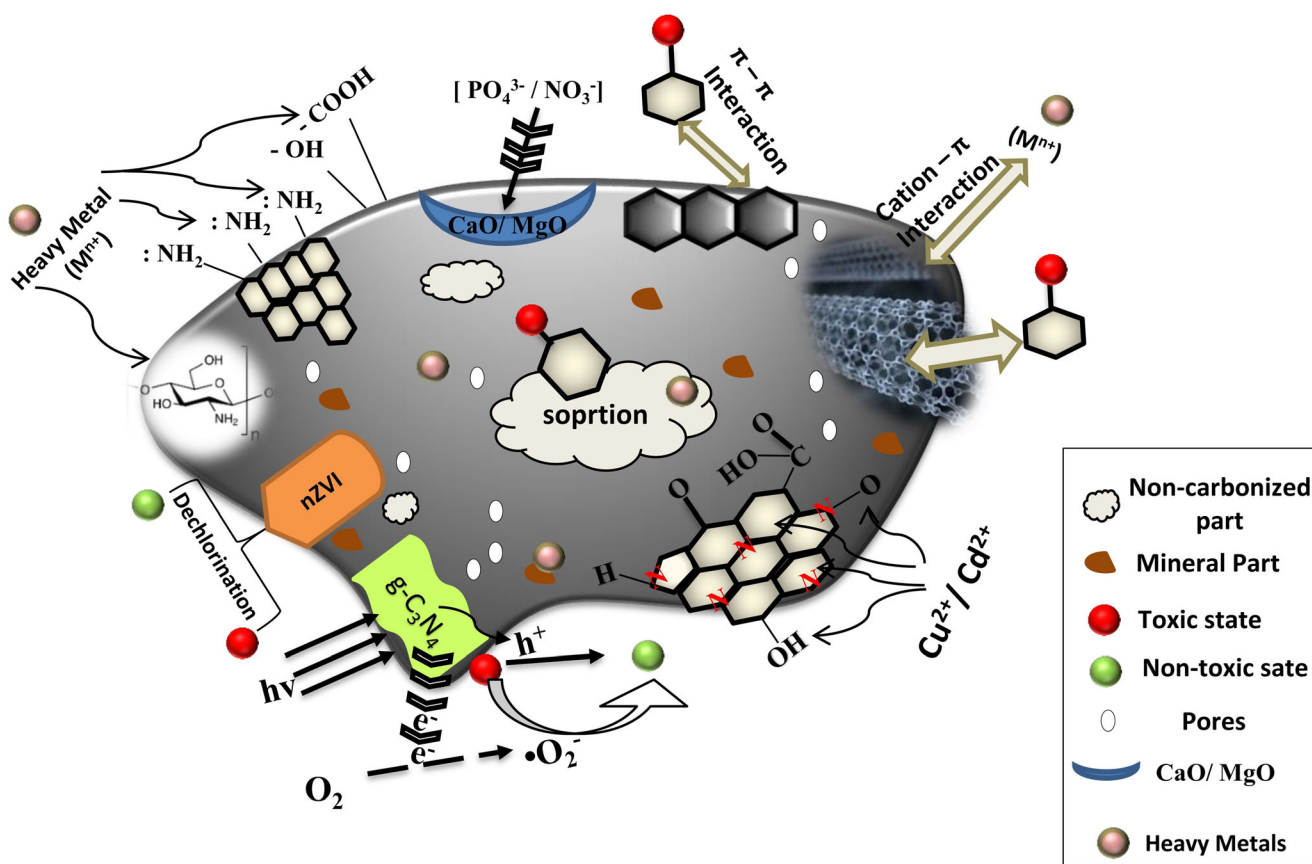


Fig. 4 Different BC modification routes and contaminants removal mechanisms

compared with uncoated BC (Zhang et al. 2014). Higher sorption of anionic DFY was possible due to the positive charge nature of the MC surface after magnesium hydroxide coating. A new engineered graphene-based BC was synthesised by treating cottonwood with graphene/pyrene-derivatives followed by annealing at 600 °C under N<sub>2</sub> atmosphere. The graphene-coated BC exhibited remarkable performance towards methylene blue adsorption, which was mainly due to strong π-π interaction present between graphene sheets available on BC surface and aromatic rings of targeted dye (Zhang et al. 2012). In addition, CNTs are also promising materials for BC modification. With high surface area and nanostructure nature, CNTs have shown remarkable efficiency for contaminant removal. Thus, the development of CNT-coated BC is a feasible method to construct economical and efficient SMs. As reported, this kind of synthesised CNT-coated BC can effectively and selectively remove both lead and sulfapyridine (SPY) in the presence of SDBS surfactant. Moreover, no obvious competition was observed between these two contaminants because of the uniform distribution of CNTs on BC surface with the assistance of SDBS (Inyang et al. 2015). Another method for BC coating regards the application of chemical vapour deposition (CVD) technique. The CVD process was found to

increase the loading of CNTs on charcoal, and the formed composite material showed significantly enhanced Cu<sup>2+</sup> sorption capacity (Saleh 2006). Even though the deposition of CNTs on BC would block the pores to some extent, increased acidic FGs introduced by CNTs enhanced the copper sorption capacity. Moreover, a comparative study between unmodified and CNT-modified both hickory (HC) and bagasse biochar (BC) for methylene blue (MB) sorption reflected that almost two times more sorption capacity was demonstrated in case of CNT-modified BC (HC, 2.4 and BC, 5.5 mg g<sup>-1</sup>) than unmodified ones (HC, 1.3 and BC, 2.2 mg g<sup>-1</sup>) (Inyang et al. 2014).

### Impregnation of functional materials into biochar

Impregnation is another important route to synthesise BC-based nano-composites which may possess catalytic and oxidative/reductive properties. Generally, impregnation can be achieved by deposition or loading of functional materials within BC porous skeleton structure. A typical example is hydrogel-biochar composite (HBC), which can be made from some waste materials such as chitosan coming from industrial sectors (Meri et al. 2018). Special properties of HBC both in terms of physical and chemical such

as hydrophilic nature and swelling ability make it a unique material (Okay 2009). HBC has gained research focus as a potential novel adsorbent for the production and application of this material in the field of wastewater and gas treatment. Modification of BC by chitosan through cross-linkage also enhances the availability of amine groups on the resulted composites, which was applied for the efficient removal of heavy metals like  $\text{Pb}^{2+}$ ,  $\text{Cu}^{2+}$ , and  $\text{Cd}^{2+}$  (Zhou et al. 2013). In addition to hydrogel-biochar, impregnation of nZVI and graphitic  $\text{C}_3\text{N}_4$  (g- $\text{C}_3\text{N}_4$ ) has also shown a great potential for BC modification because they can simultaneously perform adsorption and further degradation towards aqueous contaminants. Devi and Saroha (2014) confirmed the effectiveness of a modified route, which consisted of the impregnation of zero-valent iron (ZVI) on BC obtained through paper mill sludge followed by Ni doping, inducing unique dual property for simultaneous adsorption as well as dechlorination of pentachlorophenol. Similarly, g- $\text{C}_3\text{N}_4$ -modified BC (BC@ $\text{C}_3\text{N}_4$ ), synthesised by thermal polycondensation where BC was mixed with melamine as a precursor material, has exhibited adsorptive and photocatalytic properties. In contrast to carbon-based conventional or traditional adsorbent having saturated adsorption capacity limit, the BC@ $\text{C}_3\text{N}_4$  composite could provide a sustaining decontamination environment as a result of photocatalytic degradation of an adsorbed organic-targeted pollutant under light irradiation (Pi et al. 2015). Furthermore, the loading of  $\text{MnO}_x$  nanoparticles on BC by applying  $\text{KMnO}_4$  causes an increase in surface area and pore volume due to strong oxidising nature of the reagent applied. The optimised  $\text{MnO}_x$ -loaded BC exhibited five times more adsorption capacity for  $\text{Pb}^{2+}$  ions than that of plain BC (Faheem et al. 2016). In another study, successful sorption of oxyanions  $\text{AsO}_3^{3-}$  was carried out by using ZnO-biochar composite synthesised by  $\text{ZnCl}_2$  chemical activation of biogas residue-derived BC (Xia et al. 2016). The sorption was attributed to ligand exchange at Zn–OH active sites that give rise to Zn–O–As(III) complex formation. In a recent study, magnetic BC decorated with ZnS nanocrystals was successfully synthesised in a polyol solution. The easily removable magnetic ZnS-decorated BC provided 10 times more removal capacity of  $\text{Pb}^{2+}$  ions than the other magnetic BCs reported in the literature (Yan et al. 2014). There are many other impregnation methods for BC modification listed in Table 1, which make BC a good adsorbent for phosphate, nitrate, and oxyanions etc. Numerous varieties of contaminants including heavy metals, dyes, organic contaminants, and oxyanions are present in real wastewater stream depending upon the source. Therefore, different chemical modification routes will result in different properties of BC, which can remove a variety of contaminants simultaneously.

## Adsorptive nature of biochar for organic contaminants removal

### Functional groups of biochar and their role for adsorption

There are plenty of organic contaminants available in nature which have acute toxicity for living organisms when they enter the food chain system through water, air, and soil. For example, emerging organic contaminants which include a variety of EDCs, pharmaceuticals, and personal care products are considered most critical contaminants due to their effects on the endocrine system and interference ability with normal hormonal balance in human being as well as in wildlife (Grover et al. 2011; Zhou et al. 2009). BC shows bright potential to remove a different range of organic contaminants present in water, such as pesticides ( $0.03\text{--}23\text{ mg g}^{-1}$ ), pharmaceutical- and personal care-related products ( $0.001\text{--}59\text{ mg g}^{-1}$ ), dyes ( $3\text{--}103\text{ mg g}^{-1}$ ), furfural ( $93.5\text{--}109\text{ mg g}^{-1}$ ), and humic acid ( $60\text{ mg g}^{-1}$ ). There are different removal mechanisms including pore filling, diffusion and partitioning, electrostatic interaction, hydrophobic interaction, and hydrogen bonding (Inyang and Dickenson 2015). A comparative study for BCs derived from different feedstocks, such as lignin, cellulose, and wood, prepared at  $400\text{ }^\circ\text{C}$  and  $600\text{ }^\circ\text{C}$ , has been carried out for the purpose of nitrobenzene sorption. It was noted that both wood- and cellulose-derived BC showed almost the same composition and carbonisation degree that was much different from lignin-derived BC, suggesting that the composition of feedstock might affect BC property. The lignin BC-assisted nitrobenzene sorption was subjected to higher partition contribution to the total sorption due to lower carbonisation of lignin than the other two BCs (Li et al. 2014a). Another study revealed that extractable BCs ( $< 500\text{ }^\circ\text{C}$ ) adsorbed phenanthrene by the combined action of partition and surface adsorption due to the presence of soluble carbon. However, base modification could remove soluble carbon and thus result in only surface adsorption and an increase in sorption rate (Feng and Zhu 2017). This soluble carbon is typically made of small (poly)aromatic and aliphatic compounds, such as ketones, pyrroles, sugars, and phenols (Keiluweit et al. 2010). Therefore, these contaminants exhibited sorptive removal by the application of BC and their removal rates seem to be enhanced when the modified BC was employed compared with blank BC.

The adsorption ability of organic pollutants is closely related to the available FGs on the BC surface. The hydrophilicity of BC can be enhanced through chemical modification of surface FGs to make it more selective towards targeted pollutants. For example, the Langmuir sorption capacities ranging from  $93.5$  to  $109\text{ mg g}^{-1}$  for furfural removal was observed when the acid- or alkali-modified BCs were utilised (Li et al. 2014c; Rajapaksha et al. 2016). This was attributed to the



**Table 1** Different chemical treatments for BC modification and production conditions and their applications for targeted pollutant removal by different mechanisms involved

| Activating agent                                 | Raw biomass origin          | Biochar production, conditions | Removal capacity   | Target sorbate/pollutants      | Enhancement   | Active sites/reactive species                   | References                |
|--|-----------------------------|--------------------------------|--|--------------------------------|---|---|---------------------------|
| <b>(a) Chemical modification</b>                 |                             |                                |  |                                |   |   |                           |
| HNO <sub>3</sub> /H <sub>2</sub> SO <sub>4</sub> | Rice straw                  | 550                            | BC <sub>HNO3</sub> = 66.8<br>BC <sub>H2SO4</sub> = 65.6<br>(mg g <sup>-1</sup> ) | Phenol                         | Lactonic, quinone, alcoholic, carbonic, and carboxylic groups content increases<br>More OFGs availability | OFG presents on BC surface                      | (Yakout 2015)             |
| H <sub>2</sub> SO <sub>4</sub>                   | Rice husk                   | 450–500                        | Q <sub>max</sub> = 23.28<br>(mg g <sup>-1</sup> )                                | Tetracycline                   |   | -CO, C=O, CO <sub>2</sub> H, -OH                | (Liu et al. 2012)         |
| HCl  | Medicinal residue           | 80                             | q <sub>e</sub> = 279.3 (μg g <sup>-1</sup> )                                     | Hg <sup>0</sup>                | Increase of Cl <sup>-</sup> on surface  | Chemisorption, hydrogen bonding, -OH            | (Shen et al. 2015)        |
| H <sub>3</sub> PO <sub>4</sub>                   | Pine tree                   | 550                            | 885 mg/kg  | Fluoride                       | Surface area  | Adsorption and ion exchange                     | (Cuan et al. 2015)        |
| Nitric/citric acid                               | Hickory, cotton, and peanut | 60–100                         | hick-N = 38.1 hick-C = 30.5 (mg g <sup>-1</sup> )                                | Methylene blue                 | Increase in OFGs  | Active sites for physical adsorption            | (Ding et al. 2014)        |
| NaOH   | Bamboo charcoal             | 450                            | 2100 mg/kg   | Chloramphenicol                | Increase in OFGs + surface graphitic carbon   | π-π, -CO-COOH                                   | (Fan et al. 2010)         |
| KOH  | Rice straw                  | 550                            | BC <sub>KOH</sub> = 93.5<br>(mg g <sup>-1</sup> )                                | Phenol                         | Lactonic, quinone, alcoholic, carbonic, and carboxylic groups content increases<br>Rise in surface area   | OFGs presents on BC surface                     | (Yakout 2015)             |
| KOH  | Peanut hull                 | 800                            | Q <sub>max</sub> = 208<br>(mg g <sup>-1</sup> )                                  | Methylene blue                 |   | Physical and chemical sites                     | (Han et al. 2015b)        |
| Graphene   | Peanut shell                | 500/N <sub>2</sub> /2 h        | Q <sub>Ph</sub> = 42.2<br>Q <sub>MB</sub> = 16.1<br>(mg L <sup>-1</sup> )        | 1: Phenol<br>2: Methylene blue | Increase in S. area + pore vol.+ carbon content   | π-π stacking, electrostatic attraction          | (Chaffar and Younis 2014) |
| KOH  | Rice husk                   | 450–500                        | Q <sub>max</sub> = 58.8<br>(mg g <sup>-1</sup> )                                 | Tetracycline                   | Increase in graphitic like sheet of KOH-BC  | π-π interaction                                 | (Liu et al. 2012)         |
| KOH  | Mangostene fruit peel       | 400/N <sub>2</sub> /2 h        | Q <sub>max</sub> = 20.83<br>(mg g <sup>-1</sup> )                                | Cu <sup>2+</sup>               | Increase in surface area  | Chemical interaction                            | (Hamid et al. 2014)       |
| CH <sub>3</sub> OH                               | Rice husk                   | 450–500                        | NA <sup>a</sup>  | Tetracycline                   | -OH group, ionised moieties (-O <sup>-</sup> )/ketone moiety  | π-π electron donor acceptor interaction         | (Jing et al. 2014)        |
| H <sub>2</sub> O <sub>2</sub>                    | Rice straw                  | 550                            | Q <sub>Ph</sub> = 93.5<br>Q <sub>MB</sub> = 39.3<br>(mg g <sup>-1</sup> )        | 1: Phenol<br>2: Methylene blue | Carboxylic and phenolic groups, π electron  | -COOH, Phenolic, π-π interaction                | (Yakout 2015)             |
| CNT + surfactant                                 | Hickory chips, bagasse      | 600/1 h                        | SPL <sup>a</sup> = 86%<br>Pb = 71%   | 1:Sulfapyridine<br>2:Lead      | Graphitic sheets of CNT and BC area   | π-π + hydrophobic interaction, complexation     | (Inyang et al. 2015)      |
| nZVI/BC  | Rice husk                   | 400/2 h                        | 96.2%  | Nonylphenol                    | Increase in OFGs + surface area   | SO <sub>4</sub> <sup>2-</sup> + •OH             | (Hussain et al. 2017)     |
| N-doped BC                                       | Corn straw                  | 600/2 h                        | Q <sub>Cu</sub> = 1.63<br>Q <sub>Cd</sub> = 1.76<br>(mmol g <sup>-1</sup> )      | 1: Copper<br>2: Cadmium        | Increase in graphitic-N content   | Cation-π bonding, -OH, graphitic-N complexation | (Yu et al. 2018)          |

**Table 1** (continued)

| Activating agent                          | Raw biomass origin     | Biochar production, conditions | Removal capacity   | Target sorbate/pollutants                | Enhancement   | Active sites/reactive species   | References                |
|---|------------------------|--------------------------------|--|--|---|---|---------------------------|
| N-/O-biochar                              | Pine chip              | 300/15 min                     | $Q_{N-IBP} = 311$<br>$Q_{O-IBP} = 286$<br>( $\text{mg g}^{-1}$ )     | Naproxen, diclofenac, ibuprofen (IBP)    | Increase in S. area + pore vol. + aryl/carbohydrate FGs | $\pi$ - $\pi$ + hydrophobic + electrostatic interaction               | (Jung et al. 2015)        |
| Surfactant (TTAB <sup>a</sup> )           | Switch grass           | 450/20 min                     | Dye capacity = 1288.44<br>( $\text{mg g}^{-1}$ )                     | Reactive red 195A                        | Sorption capacity for dye boost up                      | Intraparticle diffusion process                                       | (Greluk and Hubicki 2010) |
| Surfactant (CTAB <sup>a</sup> )           | Corn stalk             | 600/3 h/without O <sub>2</sub> | $Q_{\text{max}} = 26.9$<br>( $\text{mg g}^{-1}$ )                    | Orange II                                | Ion exchange  | Electrostatic interaction   | (Mi et al. 2016)          |
| (b) Coating/impregnation                  |                        |                                |  |  |   |   |                           |
| Magnetic-ZnS-decorated BC                 | Rice Hull              | 400/5 h                        | $Q_{\text{max}} = 367.65$<br>( $\text{mg g}^{-1}$ )                  | Pb <sup>2+</sup>                         | ZnS nanocrystals incorporation                          | Diffusion reaction route  | (Yan et al. 2014)         |
| Mixture (ZnCl <sub>2</sub> + citric acid) | Sewage sludge          | 500/N <sub>2</sub> /1 h        | $Q_{\text{Phenol}} = \text{NA}$<br>$Q_{\text{B.acid}} = \text{NA}^a$ | Benzene derivatives                      | Rise in surface area                                    | Pore-filling, hydrophobic and sorption by carboxyl + SiO <sub>2</sub> | (Kong et al. 2014)        |
| Clay-biochar composite                    | Bamboo/bagasse/hickory | 600/N <sub>2</sub> /1 h        | 5 times (5×) more than pristine BC                                   | Methylene blue                           | Change in surface functionality occurs                  | Ion exchange (for clay) + electrostatic (for BC)                      | (Yao et al. 2014)         |
| Ni-ZVI-biochar                            | Paper mill sludge      | 700                            | $Q_{\text{max}} = 10$ ( $\text{mg g}^{-1}$ )                         | Pentachlorophenol                        | Impregnation of ZVI and Ni particles                    | Simultaneous adsorption and dechlorination                            | (Devi and Saroha 2015)    |
| Mg(OH) <sub>2</sub> -BC                   | Wheat straw            | 550                            | $Q_{\text{max}} = 205.5$<br>( $\text{mg g}^{-1}$ )                   | Anionic dye directly frozen yellow (DFY) | Magnesium hydroxide coating                             | Biochar OFGs + Mg(OH) <sub>2</sub> sites                              | (Zhang et al. 2014)       |

<sup>a</sup> TTAB, Tetradecyltrimethyl; CTAB, cetyltrimethylammonium bromide; SPL, sulfapyridine; NA, not available

involvement of increased acidic FGs for acid-treated BCs and increased basicity of alkaline-treated BCs, which made BC more hydrophilic in nature, and resulted in the maximum removal of furfural. However, alkali-treated BC represents higher adsorption removal capacities for furfural due to its basic nature. Furthermore, methanol-treated biochar (MeOH-BC), sulphuric acid-treated biochar (H<sub>2</sub>SO<sub>4</sub>-BC), and KOH-treated biochar (KOH-BC) have been used for the sorption of antibiotics (Liu et al. 2012). Maximum sorption of tetracycline (TC) was observed (96.5 mg g<sup>-1</sup>) for MeOH-BC obtained through rice husk when compared with other types of BCs, having 45.6% more adsorption capacity within 12 h when compared with non-treated rice husk BC or Ori-char (Jing et al. 2014). MeOH-BC is rich in ester-based and -OH than Ori-char, which favours the  $\pi$ - $\pi$  electron donor acceptor type interaction in between modified BC and TC. Methanol modification results in an increase of electron density of O atoms on BC surface with stronger basicity than O atom available on Ori-char, investigated by X-ray photoelectron spectroscopy (XPS) analysis. This was attributed to the strong electron-withdrawing nature of C=O group available on BC surface, which has a strong ability to capture electrons of -OH and other related groups. Moreover, in a recent study, N-S-doped mesoporous carbon (NSMC) was synthesised by using bone BC as the precursor. Incorporated nitrogen was present in the pyridinic, pyrrolic, and graphitic forms, while thiophene and the oxidised sulphur were the major forms of incorporated sulphur. The NSMC reflected the maximum adsorption capacity of 56.78 mg g<sup>-1</sup> for ibuprofen (IBF) (Cazetta et al. 2016). Furthermore, evaluation of successfully synthesised magnetic chicken bone biochar (MCB) for the removal of TC and rhodamine B (RhB) was tested in single- and two-stage-stirred absorbers (TSA). The optimised TSA study reflected that 33.2 g of MCB was required to attain 96% removal of TC and 22.2 g for RhB within 180 min for the applied initial concentration of 100 mg L<sup>-1</sup> (Oladipo and Ifebajo 2017).

In addition, recently carried out studies also suggested the concept of multifunctionalisation of adsorbent for the treatment of a variety of pollutants in aqueous solution, which depended upon the chemistry of adsorbent as a result of FG activation under different pH environment (Li et al. 2016; Novak et al. 2016). For example, (Faheem et al. 2018) provide a new eco-friendly way for the multifunctionalisation of BC. The surface FGs exhibited affinity for a variety of heavy metals as well as organic dyes. The amino-grafted-modified biochar (AMBC) with multifunctional groups on its surface showed adsorption-assisted decontamination of Hg<sup>2+</sup> ions from aqueous solution. Also, this AMBC showed an affinity for the efficient uptake of anionic nature Congo red dye in the presence of unwanted co-present constituents due to novel surface chemistry of AMBC as a result of -COOH and amino (-NH<sub>2</sub>) FG activation (Faheem et al. 2019). In another study, multifunctional BC was successfully applied for the selective

separation of Co<sup>2+</sup> as well as superbugs from water samples (Gao et al. 2017).

### Role of adsorption during oxidation processes induced by biochar-based catalysts

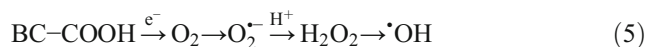
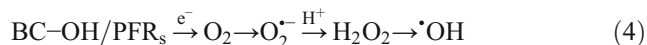
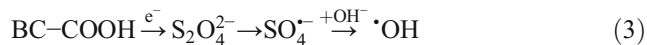
It is suggested that the higher adsorptive uptake of BC could promote the catalytic role of BC-based catalysts which finally become a cause of increase in removal efficiency of targeted pollutants. The varieties of adsorption mechanism may involve hydrophobic interactions,  $\pi$ - $\pi$  interaction, hydrogen bonding role, and electrostatic force of attraction behind the removal of targeted pollutants (Inyang et al. 2014; Tan et al. 2015; Xie et al. 2014). Pi et al. have explored the role of adsorption for the removal efficiency of MB dye by BC@C<sub>3</sub>N<sub>4</sub> composite (Pi et al. 2015). After testing different BC/melamine mass ratios, it was revealed that with increase in BC content into BC@C<sub>3</sub>N<sub>4</sub> composite, the rise in adsorption capacity and enhancement in decolourisation rate was noticed. Furthermore, bio-waste-derived nitrogen-doped sludge carbon (NC) exhibited combined adsorptive and catalytic properties for the degradation of organic pollutants in PMS activation system. The dried sludge treated with urea reagent results in increase in surface area as well as surface FGs of NC. The organic pollutants were removed by not only adsorptive but also catalytic oxidation route (Hu et al. 2019). Similarly, significant role of adsorption for the removal of safranin T was monitored when TiO<sub>2</sub>/BC catalyst was tested. For safranin T, 226.5-mg g<sup>-1</sup> adsorption capacity was achieved under UV-light irradiation condition. However, the maximum adsorption capacity of about 157.3 mg g<sup>-1</sup> (69.4% of the total removal efficiency) was obtained without any UV-light irradiation. It depicted that adsorptive potential showed slightly higher contribution for safranin T than that of photocatalytic degradation (Cai et al. 2018). The  $\cdot$ OH radicals were the main oxidising species for the degradation of safranin T. In addition, the bone char (BBC) has reflected the synergistic effect between adsorptive uptake due to higher surface area value (1024.34 m<sup>2</sup> g<sup>-1</sup>) and catalytic performance for the removal of 2,4-dichlorophenol (2,4-DCP) in PS activation system. Both radical and non-radical routes were involved behind the removal mechanism of organic pollutants (Zhou et al. 2019).

### Catalytic nature of biochar for organic contaminant removal

#### Biochar OFG-assisted catalytic activity

The BC surface contains variety of OFGs including, -OH, -COOH, lactonic, and ketonic. The extent of OFGs is directly related with the pyrolysis temperature, retention time, and variety of feedstock. These OFGs express the ability to

activate oxidising agent with generation of reactive species leading to pollutant degradation (Kemmu et al. 2018). Recently, the influence of OFGs on the adsorptive and catalytic behaviour of oxidation BC supported magnetite particles (OBC-Fe<sub>3</sub>O<sub>4</sub>) for the degradation of TC in PS system has been explored (Pi et al. 2019). It was noticed that both BC incorporated C=O and C–OH OFGs acted as electron-donating groups which would activate PS to produce SO<sub>4</sub><sup>•−</sup> reactive species and accelerate the TC decomposition. Furthermore, in another study, it was revealed that the C=O group and sp<sup>2</sup> C=C moieties also participated into catalytic degradation of ciprofloxacin (CIP) in the presence of H<sub>2</sub>O<sub>2</sub> (Luo et al. 2019). In addition, the degradation of trichloroethylene by BC loaded with nano Fe<sup>0</sup> in the presence of H<sub>2</sub>O<sub>2</sub> also suggested an interesting finding about the formation of organic radical CO<sup>•</sup> and <sup>•</sup>OH radicals as a result of BC bound C–OH FG involvement in H<sub>2</sub>O<sub>2</sub> activation through single-electron transfer route (Yan et al. 2017). Similar results have been declared such as the generation of O<sub>2</sub><sup>•−</sup> through electron transfer to the dissolved oxygen with the assistance of BC-incorporated OFGs under daylight irradiation. The generated O<sub>2</sub><sup>•−</sup> reacts with H<sup>+</sup> to generate H<sub>2</sub>O<sub>2</sub> which can further transform to <sup>•</sup>OH radicals. Moreover, hydrochar exhibits great potential to produce reactive oxygen species under day light irradiation than BC due to excessively available photoactive surface OFGs (Chen et al. 2017). Besides OFGs, the persistent free radicals (PFRs) also acted as catalytic sites for the formation of ROSs. PFRs are formed as a result of thermal decomposition of organic compounds (e.g., hydroquinones, phenols, and catechols) in the presence of different metal oxides by a chemisorption mechanism followed by electron transfer route from the adsorbate surface to the existed metal atom (Lomnicki et al. 2008; Vejerano et al. 2010). The reaction route which confirm the role of BC-associated OFGs and PFRs in order to generate ROSs is given in Eqs. (1) to (5):



### Redox properties of biochar during oxidation processes

The quinone, conjugated π-electron clouds, and hydroquinone moieties are abundantly available into condensed aromatic BC structure (Zhang et al. 2019a). These active sites are considered redox-active sites due to their ability to accept and

donate electrons simultaneously (Klöpffel et al. 2014). The ROSs, such as <sup>•</sup>OH, SO<sub>4</sub><sup>•−</sup>, <sup>1</sup>O<sub>2</sub>, and O<sub>2</sub><sup>•−</sup>, can be generated when BC is acted as an electron donor to H<sub>2</sub>O<sub>2</sub>, S<sub>2</sub>O<sub>8</sub><sup>2−</sup>, and also dissolved oxygen, respectively (Fang et al. 2015a; Wu et al. 2018).

Moreover, BC can serve as an “electron shuttle” due to its electron-accepting nature which assists to regulate electron transfer reactions (Liu et al. 2017). Due to this electron shuttle property of BC, the recombination of generated electron and holes can be avoided which enhances the degradation efficiency of targeted pollutants (Mian and Liu 2018). For example, the sulfamethoxazole (SMZ) degradation was studied by TiO<sub>2</sub> alone and TiO<sub>2</sub>/BC together. It was monitored that only 58.47% removal was achieved by pure TiO<sub>2</sub>. However, 91.27% removal efficiency was obtained by TiO<sub>2</sub> particle/BC composites which could be attributed to the BC’s electron shuttle nature that avoid the recombination of formed electrons and holes within a system (Zhang et al. 2017). Similarly, the degradation efficiency of phenol was increased due to combined effect of adsorption and photodegradation when TiO<sub>2</sub>-chitosan composite was employed to reduce in charge carrier recombination (Nawi et al. 2011).

### Biochar as catalyst support: adsorption and catalysis

#### Contaminant removal via adsorptive and catalytic processes

Many types of research indicated that <sup>•</sup>OH and SO<sub>4</sub><sup>•−</sup> radicals could be generated by the activation of H<sub>2</sub>O<sub>2</sub>, PS, and PMS through the interaction with transition metals (Anipsitakis et al. 2006; Peng et al. 2017; Tang et al. 2017). The complete life cycle of radicals consists of different stages including activation, formation, and termination or scavenging processes (Fig. 5). Many researchers have applied cobalt-based heterogeneous catalyst for the purpose of PMS activation. But severe leaching from heterogeneous cobalt-based catalyst when it is applied for PMS activation poses a threat because cobalt is considered toxic and carcinogenic in nature (Anipsitakis et al. 2005; Gerken et al. 2011; Zhang et al. 2015). To avoid such undesirable leaching of metal ions into aqueous solution, research direction has moved towards finding alternative solutions. Introduction of BC as the supporting medium for heterogeneous catalyst is considered a possible alternative which is environmentally friendly and cost-effective.

Biochar-based heterogeneous catalysts have been applied for the efficient degradation of organic pollutants as well as decolourisation of organic dyes due to unique advantages of simultaneous sorption and degradation (Tan et al. 2016). In other words, a material having remarkable adsorption capacity

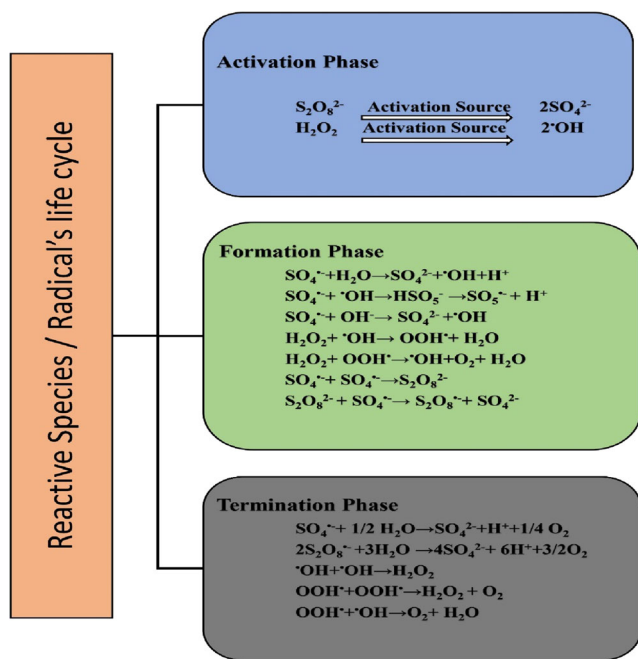


**Fig. 5** Reactive species/radical's life cycle: activation, formation, termination

is suggested for catalytic oxidation, too. BC-based composite exhibits different catalytic and oxidative/reductive properties when nanoparticles are loaded or dispersed on BC surface uniformly. As illuminated in Fig. 6, a variety of possible pathways is proposed for the generation of ROSs through different mechanisms including radical and non-radical pathways for BC-based heterogeneous catalysts (Table 2). It has been reported that dissolved organic matter (DOM) obtained from BC after 24-h agitation has the ability to oxidise As (III) and reduce Cr(VI) (Dong et al. 2014). It is also confirmed that BC can act as an “electron shuttle” in order to mediate electron transfer reactions, which directly affects the transformation pathway of contaminants present in aqueous solutions (Klүpfel et al. 2014).

Concerning about the synergistic properties of BC as the SMs for enhancing pollutant removal, a recent research study confirms the effectiveness of nZVI/BC composite for methyl orange dye removal as compared with nZVI alone or BC alone (Han et al. 2015a). The superior removal by nZVI/BC composite was attributed to the uniform dispersion of nZVI into BC matrix which enhances its reactivity as compared with less reactive aggregated nZVI. Moreover, the porous structure of BC acts as a protective layer to avoid the rapid oxidation of iron nanoparticles which lead to the passivation of nZVI or decrease in the reducing ability of iron nanoparticles. Simultaneous occurrence of both reduction and adsorption of methyl orange by BC-based nZVI was considered the main factor for decolourisation progress. Hussain et al. (2017) carried out degradation of nonylphenol by applying nZVI/BC composite for PS activation. It was observed that the

degradation rate was higher when the composite was applied than that of BC or nZVI alone. A similar trend was noticed when the trichloroethylene was degraded by nZVI/BC composite through PS oxidation process (Yan et al. 2015). It was attributed to the uniform dispersion of nZVI due to the availability of large surface area of BC as well as the presence of OFGs on BC surface which acted as an electron transfer mediator in order to promote the generation of  $\text{SO}_4^{\bullet-}$  radicals which enhanced the degradation of organic pollutants in water. Deng et al. (2018) synthesised nZVI/BC composite which activates  $\text{H}_2\text{O}_2$  in order to obtain  $\text{OH}^{\bullet}$  radical for Fenton-like removal of sulfamethazine. The research findings supported the benefits of BC as SMs for the preparation of nZVI-based heterogeneous Fenton catalyst due to many useful aspects, such as (i) avoiding the aggregation or flock formation of nZVI that affects catalyst performance, (ii) pollutant adsorption in the beginning stage that facilitates the efficient use of generated  $^{\bullet}\text{OH}$  radical, (iii) activation of  $\text{H}_2\text{O}_2$  through PFRs present on BC surface, and (iv) overcoming the passivation of nZVI with the passage of time.

Aniline degradation was investigated with rice straw biochar (RSBC) in the presence of PS. The control experiments with RSBC or PS alone were not effective due to the poor aniline removal efficiency of about 5% and < 3%, respectively. This negligible removal was due to poor adsorption and oxidation ability of RSBC and PS, respectively. In contrast, 94.1% of aniline degradation along with 52% removal of total organic carbon was achieved within 80 min when RSBC and PS were applied together (Wu et al. 2018). Radical and hole scavenging experiments as well as electron paramagnetic technique were utilised to reveal the reactive species which boosts the degradation of aniline. It was concluded that the generated hole was the main reactive species for oxidation degradation of aniline. The generation of hole was proceeded as follows: (i) the adsorption of  $\text{S}_2\text{O}_8^{2-}$  onto RSBC surface as a result of interaction with each other and (ii) the activation of  $\text{S}_2\text{O}_8^{2-}$  through electron donor groups such as  $-\text{COOH}$  and  $-\text{OH}$  available on RSBC surface along with the simultaneous generation of holes. Recently, a BC-Cu nanoparticle composite was applied for simultaneous adsorption and degradation of TC. 97.8% removal efficiency was achieved as a result of TC interaction with  $^{\bullet}\text{OH}$  generated by Cu(II)/Cu(I) redox reaction with  $\text{H}_2\text{O}_2$  and available FRs in BC matrix through electron transfer process (Fu et al. 2017).

In addition, the combined adsorption and advanced oxidation process for the treatment of refractory contaminants was also noted in sludge-derived BC/PS system. Sludge-derived biochar (SDBC) with highly porous structure and large surface area accelerated adsorption of organic contaminants onto the BC surface. The presence of abundant OFGs, as well as certain amount of Fe species in an amorphous form, remarkably boosts up the PS activation to produce various oxidative radicals in a broad pH range (Wang et al. 2017b). A recent

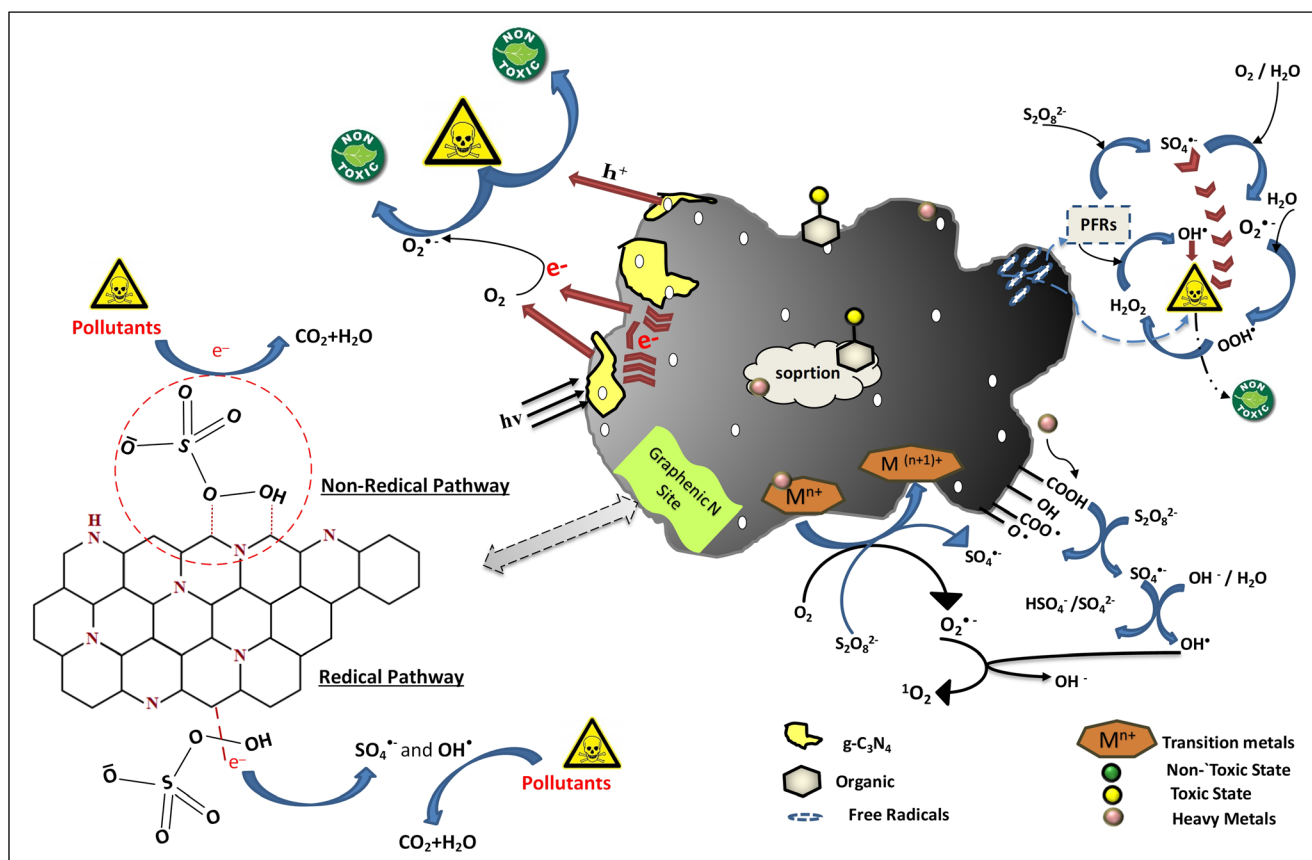


**Fig. 6** BC based heterogeneous catalysts for mineralization of contaminants through generated reactive oxygen species (ROS)

study from Chen et al. (Chen et al. 2018) confirmed the significance of the introduction of BC during  $\text{Co}_3\text{O}_4$  fabrication. Extraordinary activation for PMS and ofloxacin degradation performance were noted by applying  $\text{Co}_3\text{O}_4$  modified BC ( $\text{BC-Co}_3\text{O}_4$ ).

Park et al. (Park et al. 2018) applied Fe-impregnated sugarcane BC catalyst (FSB) for the degradation of azo dye orange G through Fenton-like reaction. Under optimum reaction conditions, maximum removal efficiency of 99.7% was obtained within 2 h. FSB exhibited good stability and reusability within consecutive 4 runs with orange G removal efficiency higher than 89.3% (Jeon et al. 2017a). Moreover, iron-doped graphitic BC was tested for the mineralisation of oestrogen through PS-activated system. The catalytic oestrogen degradation was attributed to the presence of iron-doped particles as well as porous graphitic carbonaceous structure of BC which favours the formation of both  $\text{SO}_4^{\bullet-}$  and  $\bullet\text{OH}$  oxidising species through PS activation (Zhang et al. 2019b). In another study, the utilisation of bottom ash obtained from biomass incineration for power generation was carried out for the removal of methylene blue (MB) (Liu et al. 2018). In case of bottom ash alone employed for MB removal purpose, less than 44% removal efficiency was observed which was attributed to adsorption. However, MB removal efficiency reached 100% when bottom ash was functionalised with the aid of

$\text{H}_2\text{O}_2$ . The Fenton-like reaction was suggested as the main contributor to the removal of MB due to the complex composition of bottom ash. The presence of polyaromatic moieties and FGs on unburnt carbon fraction in bottom ash as well as the expected formation of silicate during biomass combustion was thought to facilitate the activation of  $\text{H}_2\text{O}_2$  into  $\bullet\text{OH}$ .

Furthermore, not only the involvement of radical species for contaminant mineralisation but also the non-radical species contribution is an expected pathway for the degradation of targeted pollutants as shown in Fig. 6. For non-radical processes, it is proposed that the reaction initiates with temporary bonding of PMS with positively charged  $\text{sp}^2$ -hybridised carbon atom, which presents graphene-like structures of carbonaceous materials such as BCs, CNTs, AC, and MOFs. Later on, the available highly covalent  $\pi$ -electrons becomes the main cause for activating O–O bonds of PMS, resulting in direct oxidation of targeted pollutants instead of generation of free radicals (Duan et al. 2016). However, in some cases, contaminants could be degraded via both radical and non-radical processes in the same reaction system. The efficient degradation of acid orange 7 (AO7) in water has been observed through a combination of both non-radical and radical species, and not only  $\text{SO}_4^{\bullet-}$  and  $\bullet\text{OH}$  were generated but also  $^1\text{O}_2$  was formed during PMS activation by nitrogen-functionalised sludge-derived BC (Sun et al. 2017). Wang

**Table 2** Performance of varieties of BC-based catalyst for pollutants degradation through generated ROSs

| Target/pollutant  | AOPs   |                                     | Reaction parameters     |         |            | Degradation/time/radicals involve |   | References            |
|-------------------|--|-------------------------------------|-------------------------|---------|------------|-----------------------------------|---|-----------------------|
|                   | Oxidant/conc.  | Activation Source                   | Initial conc.           | pH      | Dosage g/L | Temp (°C)                         |   |                       |
| 2-Chlorobiphenyl  | H <sub>2</sub> O <sub>2</sub> /10 mM                   | Biochar                             | 10.6 mM                 | 7.4     | 1          | 25                                | 95%/2 h/•OH   | (Fang et al. 2014)    |
| Tetracycline      | H <sub>2</sub> O <sub>2</sub> /20 mM                   | Biochar-Cu composite                | 200 mg L <sup>-1</sup>  | 5.6–5.9 | 0.5        | 30                                | 97.8%/6 h/•OH   | (Fu et al. 2017)      |
| Trichloroethylene | PS/4.5 mM  | nZVI/biochar (1:5)                  | 0.15 mM                 | 6.2     | -          | 25                                | 99.4%/5 min/SO <sub>4</sub> <sup>•-</sup>                 | (Yan et al. 2015)     |
| Trichloroethylene | H <sub>2</sub> O <sub>2</sub> /1.5 mM                  | nZVI/BC                             | 0.1 mM                  | 6.2     | 1.13       | 25                                | 98.9%/30 min/•OH*   | (Yan et al. 2017)     |
| Bisphenol A       | PMS/NA <sup>a</sup>                                    | Biochar                             | -                       | 4–10    | 0.2        | -                                 | 3.21 mol BPA/mol oxidant/hole <sup>1</sup> O <sub>2</sub> | (Huang et al. 2018)   |
| 1–4Dioxane        | PS/8 mM  | nFe <sub>3</sub> O <sub>4</sub> /BC | 20 μM                   | 7       | 1          | 25                                | 98%/2 h/SO <sub>4</sub> <sup>•-</sup> + •OH               | (Ouyang et al. 2017)  |
| 4-Chlorophenol    | PS/1.85 mM   | SDBC <sup>a</sup>                   | 0.039 mM                | 6.3     | 1          | 25                                | 92.3%/100 min/SO <sub>4</sub> <sup>•-</sup> + •OH         | (Wang et al. 2017b)   |
| Aniline           | PS/90 mg L <sup>-1</sup>                               | Biochar                             | 10 mg L <sup>-1</sup>   | 3       | 0.6        | 25                                | 94.1%/80 min/hole   | (Wu et al. 2018)      |
| Nonylphenol       | PS/5 mM  | nZVI/BC                             | 20 mg L <sup>-1</sup>   | 7       | 0.4        | 25                                | 96.2%/2 h/SO <sub>4</sub> <sup>•-</sup> + •OH             | (Hussain et al. 2017) |
| <b>Dyes</b>       |  |                                     |                         |         |            |                                   |   |                       |
| Reactive red 84   | Sonication/450 W                                       | CeO <sub>2</sub> -H@BC              | 10 mg L <sup>-1</sup>   | 6.5     | 1          | -                                 | 98.5%/1 h/•OH   | (Khataee et al. 2018) |
| Methylene blue    | 4.0% H <sub>2</sub> O <sub>2</sub>                     | HBA <sup>a</sup>                    | 2000 mg L <sup>-1</sup> | -       | 4          | 25                                | 48 h/•OH  | (Liu et al. 2018)     |
| Orange G          | H <sub>2</sub> O <sub>2</sub> /0.075 g L <sup>-1</sup> | Fe-biochar                          | 100 mg L <sup>-1</sup>  | 5.5     | 0.5        | 25                                | 99.7%/2 h/•OH + OOH*                                      | (Park et al. 2018)    |
| Anthraquinone     | Sonication/300 W                                       | TiO <sub>2</sub> -BC                | 20 mg L <sup>-1</sup>   | 7       | 1.5        | -                                 | 97.5%/80 min/•OH  | (Khataee et al. 2017) |

<sup>a</sup> NA, not available; SDBC, sludge-derived BC; HBA, functionalizing bottom ash with the aid of hydrogen peroxide

et al. (2017a) reported the similar removal mechanism in case of three different kinds of organic compounds including rhodamine B (RhB), methyl orange (MO), and bisphenol-A (BPA), in which combined effects of non-radical and radical species were observed.

The doping of heteroatoms including S, P, and N into BC matrix can become a cause of change in physicochemical properties that directly effect on the catalytic as well as adsorptive properties of BC. For example, magnetic nitrogen-doped sludge biochar (MS-biochar) exhibited better catalytic property to activate peroxydisulphate (PDS) in order to produce oxidising species for the sake of TC degradation (Yu et al. 2019a). In another study, magnetic nitrogen-doped microalgae-derived carbon (Fe-N@MC) was obtained through pyrolysis route (Zou et al. 2019). This study revealed that the pyrolysis temperature played a key role to affect the  $sp^2$ -hybridised carbon structure incorporated with C=O bond that is responsible for the efficient activation of PMS to generate oxidising species. Here, the electrophilic C=O acted as an electron acceptor, and the oxidising  $^1O_2$  was obtained by electron transfer from nucleophilic PMS. Furthermore, the N-doped biochars (NBCs) obtained after urea-assisted modification process exhibited efficient sulfadiazine (SD) degradation due to superior catalytic ability to activate PDS which was attributed to available edge nitrogen moieties both pyridinic N and pyrrolic N instead of graphitic N (Wang et al. 2019). In a recent study, the oxidation BC-supported magnetite particles (OBC-Fe<sub>3</sub>O<sub>4</sub>) exhibited both excellent adsorptive uptake and catalytic activity for TC removal (Pi et al. 2019). The combined oxygen-containing FGs, carbon hybridised structure, defective sites, and the PFRs were the main contributor for PS activation.

### Oxidising species generated during biochar catalytic processes

The presence of persistent free radicals (PFRs) in BC has gained considerable research attention due to their ability to produce reactive oxygen species (ROSSs) such as  $^{\bullet}OH$ ,  $SO_4^{\bullet-}$ ,  $^1O_2$ , and  $O_2^{\bullet-}$ . Recent study confirmed the effectiveness of BC-based PFRs for organic contaminant p-nitrophenol (PNP) degradation (Yang et al. 2015). The direct contact of PNP with PFRs on BC surface results in PNP degradation. It was considered as an important contribution which was reflected by a decrease in PNP concentration in aqueous solution. Moreover, a recently performed study supported the key role of BC containing PFRs for the activation of H<sub>2</sub>O<sub>2</sub> with the main objective of organic contaminant degradation with the assistance of generated  $^{\bullet}OH$ -based ROSSs. It was revealed that a possible route for the activation of H<sub>2</sub>O<sub>2</sub> was the single-electron transfer from PFRs to H<sub>2</sub>O<sub>2</sub> (Fang et al. 2014). Fang et al. (2015a) have successfully manipulated PFRs in BC by the loading of different metals (Fe<sup>3+</sup>, Cu<sup>2+</sup>, Ni<sup>2+</sup>, and Zn<sup>2+</sup>)

and phenolic compounds (hydroquinone, catechol, and phenol) on biomass. It was observed that biomass modification does not only increase the concentration of PFRs in BC but it also results in a change in the type of PFRs formed. The results expressed that manipulation of PFRs in BC accelerates the degradation of polychlorinated biphenyl by produced  $SO_4^{\bullet-}$  interaction.

Moreover, it was revealed that increasing pyrolysis temperature causes variations in BC pore structures, shifting pH of BC reaction solutions as well as changing PFR-induced  $^{\bullet}OH$ . These were considered as the main reasons which were directly associated with the differences in the degradation rates of pollutant by the five applied BC samples (Qin et al. 2017). In addition, BC suspensions were tested for diethyl phthalate degradation in the presence of oxygen. The successful degradation was noticed due to the available PFRs in BC, which could induce  $^{\bullet}OH$  generation. It was suggested that the PFRs in BC transferred an electron to O<sub>2</sub> in order to generate  $O_2^{\bullet-}$  and H<sub>2</sub>O<sub>2</sub>, which further reacted with available PFRs to obtain  $^{\bullet}OH$  (Fang et al. 2015b). It is clear from the literature that BC redox properties totally depend upon heat treatment temperature (HTT). For example, intermediate HTTs of 400–500 °C results in the formation of engineer chars with extensive redox buffering potential by quinone/hydroquinone functionalities. On the other hand, higher HTTs of > 700 °C are considered the best conditions to form chars with conductive properties due to electron transfer through condensed aromatic sheets (Klöpffel et al. 2014). Another study demonstrated the effectiveness of hydrochar (chars form by hydrothermal carbonisation technique in the temperature range of 150–350 °C) for sulfadimidine degradation under daylight irradiation (Chen et al. 2017). Different from pyrochar (char produced at a moderate temperature of 350–700 °C through pyrolysis of biomass) obtained from the same biomass as a precursor material, hydrochar could accelerate the generation of much more H<sub>2</sub>O<sub>2</sub> and  $^{\bullet}OH$  under solar light irradiation due to the abundance of photoactive surface-oxygenated FGs. In addition, BC derived from rice husk was employed as the catalyst for the degradation of chlorobenzene in Fenton-like processes. It was concluded that oxygen reduction due to oxidation of phenolic hydroxyl groups present on BC surface assisted the formation of H<sub>2</sub>O<sub>2</sub> and  $^{\bullet}OH$  in sequence. Therefore, the availability of these hydroquinone-quinone moieties on BC accelerated the formation of ROSSs and hastened the degradation of chlorobenzene (Zhang et al. 2018a). Moreover, HNO<sub>3</sub> modified-BC reflects better catalytic properties to activate H<sub>2</sub>O<sub>2</sub> than the pristine BC applied for the degradation of CIP. It was concluded that HNO<sub>3</sub> treatment enhanced and improved the types of PFRs which promoted the generation of  $^{\bullet}OH$  species. The active sites including C=O,  $sp^2$  C=C, pyridinic-N, and PFRs of BC accelerated the production of  $^{\bullet}OH$  radicals through single-electron transfer pathway (Luo et al. 2019).

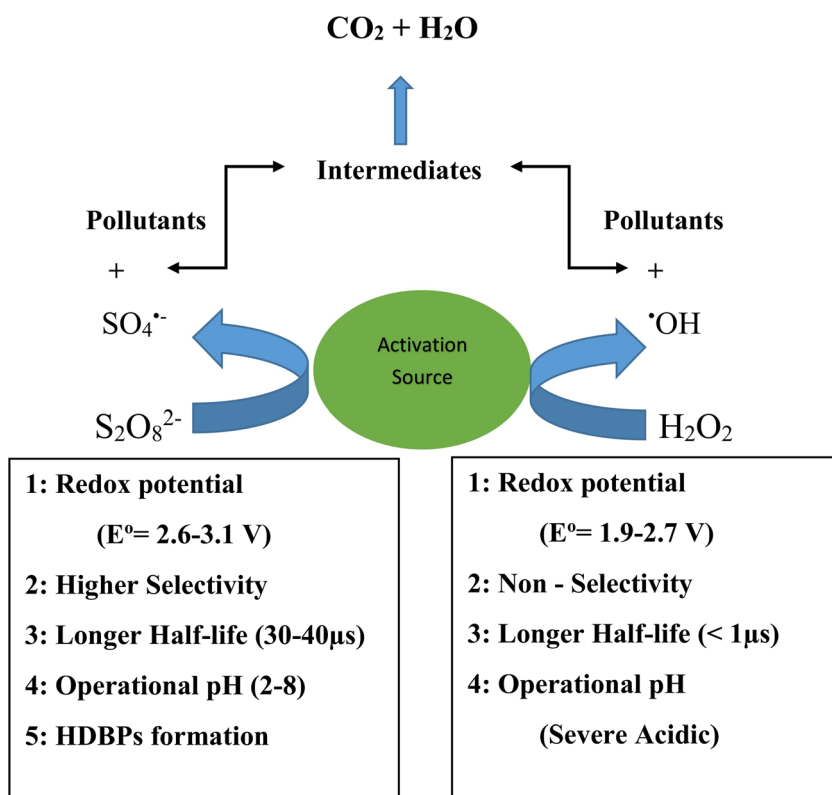


A recently carried out study gives us a new direction for photocatalytic BC preparation by using nitrogen-rich materials through pyrolysis technique. The photocatalytic BCs having graphitic carbon nitride (g-C<sub>3</sub>N<sub>4</sub>) structure were prepared by using urea, glycine, L(+)-arginine, and nitrogen-rich soybean puree (Jeon et al. 2017b). From all these materials applied, only urea-based BC exhibited photocatalytic ability due to the presence of the g-C<sub>3</sub>N<sub>4</sub> structure. The urea-based photocatalyst BC was further applied for the oxidation of orange G. Despite the urea BC photocatalytic catalytic, lower oxidation reaction rate of about 0.0043 min<sup>-1</sup> was observed for orange G. In order to enhance the oxidation rate of orange G, PS was added into the reaction system. The oxidation rate of orange G increased up to 0.0349 min<sup>-1</sup> as a result of the simultaneous application of urea-derived BC and PS. However, the lowest oxidation rate of orange G was 0.0004 min<sup>-1</sup> in case of PS only. Synergetic effects between BC and PS accelerated the generation of SO<sub>4</sub><sup>•-</sup> which resulted in complete oxidation of the partially oxidised intermediates of orange G. Moreover, for the mineralisation of bisphenol A, sludge-derived BC-based catalyst was applied to activate peroxydisulphate in order to generate <sup>1</sup>O<sub>2</sub> reactive species. It was suggested that metals found in the sludge precursor played an important role for the formation of active sites during raw sludge pyrolysis stage (Huang et al. 2018).

In last decade, SO<sub>4</sub><sup>•-</sup>-involved AOP has been intensively studied due to its ability to decompose a wide range of

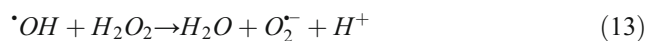
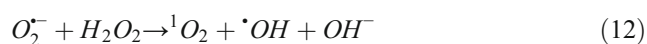
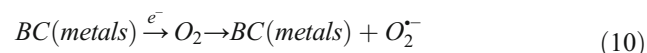
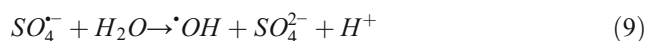
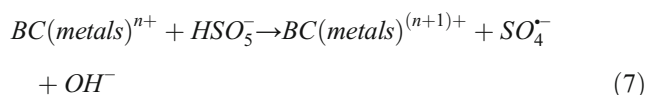
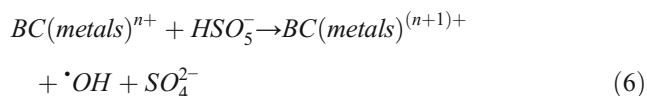
contaminants, including herbicides (Guan et al. 2013), perfluoroalkyl compounds (Lee et al. 2009), polycyclic aromatic hydrocarbons (Usman et al. 2012), petroleum hydrocarbons (Yen et al. 2011), and polychlorinated biphenyl (Rastogi et al. 2009b). SO<sub>4</sub><sup>•-</sup> radicals not only possess a relatively high one-electron reduction potential of about 2.5–3.1 V compared with <sup>•</sup>OH radicals (acidic range, 2.7 V; neutral solution, 1.8 V), but also are more selective for a broad spectrum of contaminants (Fig. 7). PMS and PS are typical precursors for the production of SO<sub>4</sub><sup>•-</sup> radicals. PMS/PS are more stable in nature than H<sub>2</sub>O<sub>2</sub>, thus favouring their transport to a greater distance in the sub-surface (Liang et al. 2007; Liang et al. 2003). In general, SO<sub>4</sub><sup>•-</sup> has a longer half-life (30–40 μs) and wide operation pH range than <sup>•</sup>OH, and is more effective for pollutant degradation due to better mass transfer and more sufficient interaction between generated radicals and target pollutants. In the case of <sup>•</sup>OH radicals, short half-life (< 1 μs) and a narrow operating pH condition in severe acidic condition are the main constraints. As a result, the SO<sub>4</sub><sup>•-</sup>-driven degradation route may result in a better mineralisation than that of <sup>•</sup>OH (Liang et al. 2007). SO<sub>4</sub><sup>•-</sup> initiates oxidation via electron transfer, electrophilic radical addition, and hydrogen abstraction (Neta et al. 1977; Tully et al. 1981). Due to this electrophilic nature, SO<sub>4</sub><sup>•-</sup> is prone to directly attack electron-donating FGs, such as unsaturated bonds, -NH<sub>2</sub>, pi-electron moieties (π-electrons) available on aromatic molecules, -OH, and alkoxy (-OR) groups. In case of SO<sub>4</sub><sup>•-</sup> interaction with electron-

Fig. 7 Comparison between hydroxyl and sulfate-based radicals



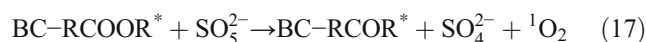
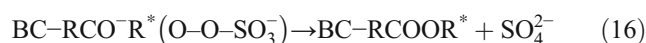
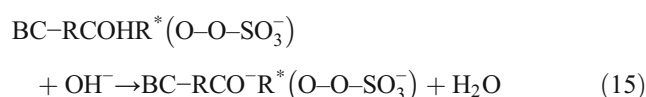
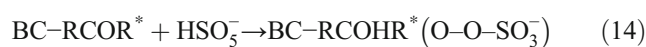
withdrawing FGs such as C=O and nitro (–NO<sub>2</sub>) substitutes, reactions would be generally slower (Luo et al. 2017; Xiao et al. 2015).

Moreover, the generated SO<sub>4</sub><sup>•−</sup> radicals can be transformed into OH<sup>•</sup> species as a result of redox reaction occurred between the available SO<sub>4</sub><sup>•−</sup> radicals and OH<sup>−</sup>/H<sub>2</sub>O as shown in Eqs. (6) to (9). In addition, the expected route for the generation of <sup>1</sup>O<sub>2</sub> in the presence of H<sub>2</sub>O<sub>2</sub> is expressed in Eqs. (10) to (13) (Kim et al. 2018; Yu et al. 2019b):



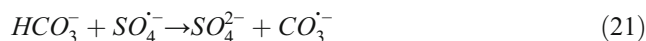
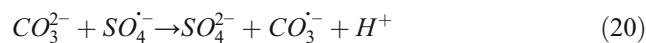
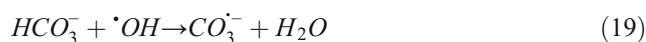
Biochar-incorporated surface FGs like ketonic groups could act as active site as catalyst in order to activate PMS for the degradation of pollutants under consideration. Recently, sludge BC-based catalyst was tested for the effective degradation of bisphenol A (BPA) by the assistance of ROSs generated in system through the activation of PMS oxidant (Huang et al. 2018). It was elucidated that <sup>1</sup>O<sub>2</sub> was the main ROSs involved for the mineralisation of BPA. The formation of epoxy structure was the key route to obtain <sup>1</sup>O<sub>2</sub> in ketone-catalysed PMS decomposition pathway as shown in Eqs. (14) to (17) as well as expressed in Fig. 6. Similar results can be found when CNTs were employed to activate PS oxidant for the catalytic degradation of 2,4-dichlorophenol (2,4-DCP). It was deduced that none of the SO<sub>4</sub><sup>•−</sup> and OH<sup>•</sup> were monitored in the system, just <sup>1</sup>O<sub>2</sub> was detected by electron paramagnetic resonance spectrometry (EPR) indicating the non-radical pathway (Cheng et al. 2017). Furthermore, increasing research work revealed that <sup>1</sup>O<sub>2</sub> is the main ROSs for the degradation of targeted pollutants along with small contribution from OH<sup>•</sup> and O<sub>2</sub><sup>•−</sup>. These findings depict that these ROSs generated sequentially rather than the simultaneous production (Carrier et al. 2018; Kim et al. 2018). The nitrogen-doped graphitic biochars (N-BCs) also demonstrated excellent catalytic activity for the degradation of variety of organic pollutants, including BPA, SMZ, orange G, and phenol by activating PDS oxidant. The N-BCs treated at 900 °C reflected higher

degradation rate for pollutants via the non-radical oxidative pathway. In contrast, radical-based oxidative route was noticed in the PDS system when N-BCs were produced at 400 °C due to the presence of PFRs (Zhu et al. 2018). In addition, release of DOM from BC suspension was noticed during UV irradiation. It was revealed that DOM extracted from BC significantly contributed in the formation of ROSs including OH<sup>•</sup> and <sup>1</sup>O<sub>2</sub> in the BC/UV system. It was also confirmed that quinone and quinone-like active sites present into BC matrix also responsible for the generation of <sup>1</sup>O<sub>2</sub> under light (Fang et al. 2017). Similarly, Fu et al. suggested that dissolved black carbon extracted from BC matrix was the main photoactive component present in BC-derived DOM, which accelerated the generation of O<sub>2</sub><sup>•−</sup> and <sup>1</sup>O<sub>2</sub> during irradiation other than carboxyl/ketonic/ester/quinone-based active sites of BC (Fu et al. 2016):



### Effect of water impurities on AOP efficiency

Generally, the most common water impurities include bicarbonate, carbonate, chloride, reaction intermediates, and solutes, which can act as radical scavengers. The presence of these water impurities results in both positive and negative impacts on Fenton-like reaction process efficiency, which is directly associated with their threshold concentration level. Carbonates and bicarbonate anions are normally found in water and wastewater streams. These anions have a tendency to react with available free radicals (so-called scavenging), which have adverse effects on both the rate of pollutant degradation and the oxidant decomposition (Asghar et al. 2015). Interaction of carbonates or bicarbonate anions with OH<sup>•</sup> or SO<sub>4</sub><sup>•−</sup> results in the formation of carbonate radicals (Eqs. (18) to (21)).



It is stated that the newly generated carbonate radicals have sufficient reduction potential (1.63 V) for organic contaminant degradation (Bennedsen et al. 2012). However, an overall adverse effect on organic pollutant degradation performance was

observed when carbonate radicals were produced as a result of carbonate and bicarbonate anion interaction with  $\text{SO}_4^{\bullet-}$  radicals in a PS-activated system (Liang et al. 2006). The presence of carbonate and bicarbonate anions at neutral pH did not affect the degradation efficiency. However, negative impact of carbonates on AOPs was dominant at higher pH value due to carbonate radical formation in alkaline pH range (Asghar et al. 2015). In addition, in the case of bicarbonate ions, it was noticed that the inhibitory effect was enhanced when the bicarbonate ion concentration rose from 1 to 100 mM (Wang et al. 2000). This trend clearly shows that the presence of bicarbonate ion results in  $\text{SO}_4^{\bullet-}$  radical scavenging. The weakness of AOP efficiencies could be due to the formation of aqueous complexes or solid precipitates during the interaction between carbonate and metal surfaces (Keen et al. 2014). In opposition to the above findings, some studies declared the positive effect of carbonate and bicarbonate ions on the pollutant degradation (Gebel et al. 2010; Yang et al. 2011). This enhanced degradation rate could originate from the involvement of carbonate radicals which might exhibit higher selectivity towards targeted pollutants compared with  $\cdot\text{OH}$  and  $\text{SO}_4^{\bullet-}$ . Therefore, it is a challenging task to identify specific threshold concentration while consider other system variables.

The presence of chloride ions ( $\text{Cl}^-$ ) in water and wastewater system has drawn much more attention due to their ability to form highly toxic chlorinated by-products as  $\text{Cl}^-$  interacts with  $\text{OH}^\bullet$  and  $\text{SO}_4^{\bullet-}$  radicals (Toor and Mohseni 2007). The exact role of  $\text{Cl}^-$  ions is still unclear due to both complementary and inhibitory effects on contaminant degradation as reported in different literatures. For example, the presence of  $\text{Cl}^-$  ions was considered to be beneficial during PMS activation, which was reflected by the enhancement of azo dye degradation (Yang et al. 2011). However, Chan and Chu reported the inhibitory effects of  $\text{Cl}^-$  because of the generation of quite weak radicals  $\text{Cl}^\bullet$  and  $\text{Cl}_2^{\bullet-}$  as a result of scavenging of strong  $\text{SO}_4^{\bullet-}$  radicals by  $\text{Cl}^-$  ions (Chan and Chu 2009). Moreover,  $\text{Cl}^-$  ions could also exert both complementary and inhibitory effects as reported in Co/PMS system for azo dye degradation (Wang et al. 2011). In case of trichloroethylene (TCE) degradation, the presence of  $\text{Cl}^-$  ions with concentration below 0.2 M did not affect TCE removal, while decreased TCE removal was noticed in presence of high  $\text{Cl}^-$  ion concentrations ( $>0.2$  M) (Liang et al. 2006). Therefore, literature survey confirmed that there is a specific threshold concentration level of  $\text{Cl}^-$  ions above which inhibitory effects become dominant. Figure 8 a provides details of the generation of  $\text{Cl}^\bullet$  and  $\text{Cl}_2^{\bullet-}$  radicals and formation pathway of undesired compounds having carcinogenic nature.

Based on the optimisation concept, an adequate amount of both activating agent and oxidant is critical to obtain high degradation efficiency in AOPs. The decrease in AOP efficiency was ascribed to the combined effect of self-

destruction of generated radicals, termination mechanisms, and scavenging as shown in Fig. 5. For example, various concentration of fulvic acid and tert-butanol was added into the UV/ $\text{H}_2\text{O}_2$  system with the main objective to study the effect of scavengers on already available  $\cdot\text{OH}$  radicals (Méndezdiaz et al. 2010). It was confirmed that the addition of this reagent diminished the degradation process as a result of  $\cdot\text{OH}$  scavenging. Another study depicted that higher degradation of 2-chlorobiphenyl was achieved under the optimum Fe (II) to PMS molar ratio of 1:1. Further increase in Fe(II) to PMS molar ratio lead to side reactions which were reflected by the utilisation of most of the generated  $\text{SO}_5^{\bullet-}$  radicals in the side reactions (Rastogi et al. 2009a). Moreover, decaying or termination of generated  $\cdot\text{OH}$  and  $\text{SO}_4^{\bullet-}$  radicals due to the abundance of these radical species accelerated the formation of  $\text{H}_2\text{O}_2$  and  $\text{S}_2\text{O}_8^{2-}$ , respectively (Criquet and Leitner 2009).

### Formation and control of halogenated intermediates in biochar-based AOPs

Despite many advantages of SR-AOPs over  $\cdot\text{OH}$ -based AOPs as briefly discussed in Fig. 7, there are several limitations which should be considered in order to avoid secondary pollution. Figure 8 a describes the possible routes by which the water stream containing  $\text{Cl}^-/\text{Br}^-$  ions results in the formation of unwanted chlorate ( $\text{ClO}_3^-$ ) and bromate ( $\text{BrO}_3^-$ ) through  $\text{SO}_4^{\bullet-}$ -assisted oxidation reactions in SR-AOPs. Both  $\text{ClO}_3^-$  and  $\text{BrO}_3^-$  are acutely toxic in nature. The maximum permitting limit of  $\text{BrO}_3^-$  in drinking water is 10  $\mu\text{g}/\text{L}$  due to its carcinogenic nature. Commonly, the reaction starts when  $\text{SO}_4^{\bullet-}$  reacts with available  $\text{X}^-$  ( $\text{X} = \text{Cl}/\text{Br}$ ) in water to produce  $\text{X}^\bullet$  which are further converted to  $\text{HOX}$  and finally  $\text{XO}_3^-$  as HDBPs [27]. In the case of PS, precursors involved in the formation of the final product are  $\text{X}^-$ ,  $\text{X}_2$ , and  $\text{HOX}$  (Liu et al. 2015).

There are potential solutions available in order to alleviate the generation of  $\text{XO}_3^-$  in the SR-AOPs system: (i) involvement of secondary treatment facility attached inline after  $\text{SO}_4^{\bullet-}$  oxidation, (ii) pH adjustment and chemical addition to suppress the formation rate of  $\text{XO}_3^-$  through kinetic control, (iii) implementation of heterogeneous catalysts. Due to high cost concern, the employment of adsorption-based removal of  $\text{XO}_3^-$  and HDBPs through biological AC or AC is not feasible (Kirisits et al. 2000; Toor and Mohseni 2007). In case of pH adjustment to suppress the formation rate of  $\text{XO}_3^-$ , higher pH seems to be a beneficially possible solution and is advantageous to heterogeneous catalyst/PMS systems both in terms of treatment efficiency and heterogeneous catalyst stability. The  $\text{Cl}^\bullet$  transformed into  $\text{ClO}_3^-$  as pH was lower than 5. When  $\text{pH} > 5$ ,  $\cdot\text{OH}$  formed due to the reaction between  $\text{Cl}^\bullet$  and water. Similarly, it was reported that during ozonation process,  $\text{BrO}_3^-$  generated via  $\text{SO}_4^{\bullet-}$  oxidation decreased up to 90% when pH rose from 7 to 9, which was attributed to the quite slow transformation of  $\text{Br}^\bullet$  into  $\text{BrO}_3^-/\text{HOBr}$  (Li et al. 2015). Addition of carbonate/



advantages, such as low cost and adsorption affinity for organic pollutants due to available OFGs. The FGs available on BC surfaces such as  $-\text{COOH}$ ,  $\text{C}=\text{O}$ , and  $-\text{OH}$  groups are able to activate PS or PMS with production of  $\text{SO}_4^{\bullet-}$  radicals (Duan et al. 2015; Wang et al. 2016c). Regarding the future application of BC for advanced oxidation processes, there are several perspectives should be considered.

- (1) Until now, most of the works are limited to the laboratory stage and theory-based. Few reports can be found regarding large-scale applications of modified or engineered BC. From industrial perspective, large-scale production and application of BC for a specific purpose are still in its infancy or initial stage and require more studies to design and develop most efficient and simple routes for mass production of BC materials at low cost.
- (2) It is important to develop proper route sequencing in order to avoid undesired effects during BC-based catalyst synthesis to get maximum return with the minimum demerit. For example, loading nano-sized particles on BC can give the superior catalytic property of the composite material on the one hand, but cause smaller BC surface area and pore volume on the other hand.
- (3) Biochar modification methods are key factors for tailoring BC surface properties. Chemical-based modification could be considered more beneficial because of the high surface area, high porosity, and especially the availability of more OFGs. However, the use of strong oxidants, strongly acidic and basic conditions during BC modification may pose a threat to the environment due to the risks of secondary pollution. Environmental friendly reagents such as  $\text{H}_2\text{O}_2$  and acetic, citric, and tartaric acids have been successfully employed for BC modification purposes (Huff and Lee 2016; Sun et al. 2015; Zhu et al. 2008). Thus, future studies should focus on the development as well as the application of less cost and green chemical reagents for the synthesis of modified BC.
- (4) It is also recommended that the multifunctionalisation of BC could boost its application in a versatile manner, for example, detoxification of aqueous environments as well as for soil remediation purposes depending upon the targets or goals to achieve. Moreover, BC incorporated with multiple functionalities can provide attractive applications for environmental purification (Novak et al. 2016; Ok et al. 2015).
- (5) It is suggested that further research work should be focused in the development of heterogeneous catalyst composites by using BC as SMs with attractive feature of adsorptive property for unwanted HDBPs and  $\text{XO}_3^-$  (Kearns et al. 2015).
- (6) Future research work should be done in the direction to explore the potential of BC-derived DOM to minimise the generation of non-desired HDBPs and  $\text{XO}_3^-$ .
- (7) Further extensive research works are required in order to grasp the details of fundamental mechanisms consisting of radical pathways and non-radical pathways as a result of synergetic effects produced between supporting media and active species and their activation ability in case of  $\text{H}_2\text{O}_2$ , PMS, and PS (Fang et al. 2017; Fu et al. 2016).
- (8) Future study should be carried out in order to make BC-based composites which have dual benefit nature of adsorption as well as a visible light photocatalytic activity to activate PMS/PS/ $\text{H}_2\text{O}_2$  to obtain reactive species  $^{\bullet}\text{OH}$ ,  $\text{SO}_4^{\bullet-}$ ,  $\text{O}_2^{\bullet-}$ , and  $^1\text{O}_2$ .
- (9) Further research is needed for the development of BC-based catalyst having dual properties for the sorption of organic pollutants as well as heavy metals at the same time before further treatment in real wastewater streams.
- (10) Research advancements are still required especially for BC production/modification refers to “desired application concern” or “reaction oriented”. Therefore, future BC synthesis/modification protocols must focus on reaction characteristics such as hydrophobic nature and molecular size of applied reactants, generated intermediates, and final products to get desirable outcomes.
- (11) Management of spent BC should be considered in order to avoid secondary pollution. Precisely, phosphate-, ammonium-, and nitrate-laden BC could be used as soil amendments as a slow-release fertiliser (Yao et al. 2013). However, in the case of BC loaded with toxic pollutants, desorption/regeneration studies must be carried out for resource recovery.

## Conclusions

Current investigations compel that BC-based heterogeneous Fenton catalyst can be considered an environmentally sustainable alternative to replace AC for treating organic contaminants present in wastewater streams. Use of chemically modified BC as SMs for Fenton catalyst to achieve dual functions of adsorption and degradation simultaneously is the best choice to implement. It is concluded that  $^{\bullet}\text{OH}$ ,  $\text{SO}_4^{\bullet-}$ ,  $^1\text{O}_2$ , and  $\text{O}_2^{\bullet-}$  are the main ROSs involved in the degradation of organic contaminants. Moreover, the presence of scavenger ions (carbonates, bicarbonates, chlorides, reaction intermediates, and solutes) plays an important role in determining the degradation efficiency of AOPs.

**Funding information** This research is financed by the Hubei Natural Science Foundation (2018CFB262) and Fundamental Research Funds for the Central Universities, China University of Geosciences (Wuhan) (no. CUG170646) and a grant from the future R&D Program (2E28020) of Korea Institute of Science and Technology (KIST).

## References

- Anipsitakis GP, Stathatos E, Dionysiou DD (2005) Heterogeneous activation of oxone using Co<sub>3</sub>O<sub>4</sub>. *J Phys Chem B* 109:13052–13055. <https://doi.org/10.1021/jp052166y>
- Anipsitakis GP, Dionysiou DD, Gonzalez MA (2006) Cobalt-mediated activation of peroxymonosulfate and sulfate radical attack on phenolic compounds. Implications of chloride ions. *Environ Sci Technol* 40:1000–1007
- Asghar A, Raman AAA, Daud WMAW (2015) Advanced oxidation processes for in situ production of hydrogen peroxide/hydroxyl radical. <https://doi.org/10.1021/jclevpro.2014.09.010>
- Azargohar R, Dalai AK (2008) Steam and KOH activation of biochar: experimental and modeling studies. *Microporous Mesoporous Mater* 110:413–421. <https://doi.org/10.1016/j.micromeso.2007.06.047>
- Bautista P, Mohedano A, Casas J, Zazo J, Rodriguez J (2010) Oxidation of cosmetic wastewaters with H<sub>2</sub>O<sub>2</sub> using a Fe/γ-Al<sub>2</sub>O<sub>3</sub> catalyst. *Water Sci Technol* 61:1631–1636
- Bennedsen LR, Muff J, Sogaard EG (2012) Influence of chloride and carbonates on the reactivity of activated persulfate. *Chemosphere* 86:1092–1097
- Boix C et al (2016) Behaviour of emerging contaminants in sewage sludge after anaerobic digestion. *Chemosphere* 163:296–304. <https://doi.org/10.1016/j.chemosphere.2016.07.098>
- Cai X et al (2018) Titanium dioxide-coated biochar composites as adsorptive and photocatalytic degradation materials for the removal of aqueous organic pollutants. *J Chem Technol Biotechnol* 93:783–791
- Carrier A NC, Oakley D, Chen Y, Oakes K, MacQuarrie S, Xu Zhang (2018) Selective generation of singlet oxygen in chloride accelerated copper fenton chemistry. [https://chemrxiv.org/articles/Selective\\_Generation\\_of\\_Singlet\\_Oxygen\\_in\\_Chloride\\_Accelerated\\_Copper\\_Fenton\\_Chemistry/7364225/1](https://chemrxiv.org/articles/Selective_Generation_of_Singlet_Oxygen_in_Chloride_Accelerated_Copper_Fenton_Chemistry/7364225/1). Accessed 4 Dec 2019
- Cazetta AL, Martins AC, Pezoti O, Bedin KC, Beltrame KK, Asefa T, Almeida VC (2016) Synthesis and application of N–S-doped mesoporous carbon obtained from nanocasting method using bone char as heteroatom precursor and template. *Chem Eng J* 300:54–63
- Chan KH, Chu W (2009) Degradation of atrazine by cobalt-mediated activation of peroxymonosulfate: different cobalt counterions in homogenous process and cobalt oxide catalysts in photolytic heterogeneous process. *Water Res* 43:2513–2521
- Chen C, Li X, Tong Z, Li Y, Li M (2014) Modification process optimization, characterization and adsorption property of granular fir-based activated carbon. *Appl Surf Sci* 315:203–211
- Chen N, Huang Y, Hou X, Ai Z, Zhang L (2017) Photochemistry of hydrochar: reactive oxygen species generation and sulfadimidine degradation. *Environ Sci Technol* 51:11278–11287
- Chen L, Yang S, Zuo X, Huang Y, Cai T, Ding D (2018) Biochar modification significantly promotes the activity of Co<sub>3</sub>O<sub>4</sub> towards heterogeneous activation of peroxymonosulfate. *Chem Eng J* 354:856–865
- Cheng X, Guo H, Zhang Y, Wu X, Liu Y (2017) Non-photochemical production of singlet oxygen via activation of persulfate by carbon nanotubes. *Water Res* 113:80–88
- Chi GT, Churchley J, Huddersman KD (2013) Pilot-scale removal of trace steroid hormones and pharmaceuticals and personal care products from municipal wastewater using a heterogeneous Fenton's catalytic process. *Int J Chem Eng* 2013:1–10. <https://doi.org/10.1155/2013/760915>
- Criquet J, Leitner NK (2009) Degradation of acetic acid with sulfate radical generated by persulfate ions photolysis. *Chemosphere* 77:194–200
- Dantas T, Mendonca V, Jose H, Rodrigues A, Moreira R (2006) Treatment of textile wastewater by heterogeneous Fenton process using a new composite Fe<sub>2</sub>O<sub>3</sub>/carbon. *Chem Eng J* 118:77–82
- Deng D, Peng L, Guan M, Kang Y (2014) Impact of activation methods on persulfate oxidation of methyl tert-butyl ether. *J Hazard Mater* 264:521–528
- Deng J et al (2018) Nanoscale zero-valent iron/biochar composite as an activator for Fenton-like removal of sulfamethazine. *Sep Purif Technol* 202:130–137. <https://doi.org/10.1016/j.seppur.2018.03.048>
- Devi P, Saroha AK (2014) Synthesis of the magnetic biochar composites for use as an adsorbent for the removal of pentachlorophenol from the effluent. *Bioresour Technol* 169:525–531
- Devi P, Saroha AK (2015) Simultaneous adsorption and dechlorination of pentachlorophenol from effluent by Ni–ZVI magnetic biochar composites synthesized from paper mill sludge. *Chem Eng J* 271:195–203
- Ding ZH, Hu X, Zimmerman AR, Gao B (2014) Sorption and cosorption of lead (II) and methylene blue on chemically modified biomass. *Bioresour Technol* 167:569–573. <https://doi.org/10.1016/j.biortech.2014.06.043>
- Dong X, Ma LQ, Gress J, Harris W, Li Y (2014) Enhanced Cr (VI) reduction and As (III) oxidation in ice phase: important role of dissolved organic matter from biochar. *J Hazard Mater* 267:62–70
- Duan XG, Sun HQ, Kang J, Wang YX, Indrawirawan S, Wang SB (2015) Insights into heterogeneous catalysis of persulfate activation on dimensional-structured nanocarbons. *ACS Catal* 5:4629–4636. <https://doi.org/10.1021/acscatal.5b00774>
- Duan X, Ao Z, Zhou L, Sun H, Wang G, Wang S (2016) Occurrence of radical and nonradical pathways from cocatalysts for aqueous and nonaqueous catalytic oxidation. *Appl Catal B Environ* 188:98–105
- Erdinc N, Gokturk S, Tuncay M (2010) A study on the adsorption characteristics of an amphiphilic phenothiazine drug on activated charcoal in the presence of surfactants. *Colloid Surf B* 75:194–203. <https://doi.org/10.1016/j.colsurfb.2009.08.031>
- Faheem YH, Liu J, Shen J, Sun X, Li J, Wang L (2016) Preparation of MnO<sub>x</sub>-loaded biochar for Pb<sup>2+</sup> removal: adsorption performance and possible mechanism. *J Taiwan Inst Chem Eng* 66:313–320
- Faheem, Bao JG, Zheng H, Tufail H, Irshad S, Du JK (2018) Adsorption-assisted decontamination of Hg(II) from aqueous solution by multifunctionalized comcob-derived biochar. *RSC Adv* 8:38425–38435. <https://doi.org/10.1039/c8ra06622a>
- Faheem, Du JK, Bao JG, Hassan MA, Irshad S, Talib MA (2019) Multifunctional biochar novel surface chemistry for efficient capture of anionic Congo red dye: behavior and mechanism. *Arab J Sci Eng* 44:10127–10139. <https://doi.org/10.1007/s13369-019-04194-x>
- Fan Y, Wang B, Yuan S, Wu X, Chen J, Wang L (2010) Adsorptive removal of chloramphenicol from wastewater by NaOH modified bamboo charcoal. *Bioresour Technol* 101:7661–7664
- Fang G, Gao J, Liu C, Dionysiou DD, Wang Y, Zhou D (2014) Key role of persistent free radicals in hydrogen peroxide activation by biochar: implications to organic contaminant degradation. *Environ Sci Technol* 48:1902–1910
- Fang G, Liu C, Gao J, Dionysiou DD, Zhou D (2015a) Manipulation of persistent free radicals in biochar to activate persulfate for contaminant degradation. *Environ Sci Technol* 49:5645–5653
- Fang G, Zhu C, Dionysiou DD, Gao J, Zhou D (2015b) Mechanism of hydroxyl radical generation from biochar suspensions: implications to diethyl phthalate degradation. *Bioresour Technol* 176:210–217
- Fang GD, Liu C, Wang YJ, Dionysiou DD, Zhou DM (2017) Photogeneration of reactive oxygen species from biochar suspension for diethyl phthalate degradation. *Appl Catal B Environ* 214:34–45. <https://doi.org/10.1016/j.apcatb.2017.05.036>
- Feng Z, Zhu L (2017) Sorption of phenanthrene to biochar modified by base. *Front Environ Sci Eng* 12:1

- Fu H et al (2016) Photochemistry of dissolved black carbon released from biochar: reactive oxygen species generation and phototransformation. *Environ Sci Technol* 50:1218–1226
- Fu D, Chen Z, Xia D, Shen L, Wang Y, Li Q (2017) A novel solid digestate-derived biochar-Cu NP composite activating H<sub>2</sub>O<sub>2</sub> system for simultaneous adsorption and degradation of tetracycline. *Environ Pollut* 221:301–310. <https://doi.org/10.1016/j.envpol.2016.11.078>
- Fujita I, Tomooka J, Sugimura T (1991) Sorption of anionic surfactants with wood charcoal. *Bull Chem Soc Jpn* 64:738–740
- Gao H, Chen J, Zhang Y, Zhou X (2016) Sulfate radicals induced degradation of triclosan in thermally activated persulfate system. *Chem Eng J* 306:522–530
- Gao Y, Pramanik A, Begum S, Sweet C, Jones S, Alamgir A, Ray PC (2017) Multifunctional biochar for highly efficient capture, identification, and removal of toxic metals and superbugs from water samples. *ACS Omega* 2:7730–7738. <https://doi.org/10.1021/acsomega.7b01386>
- Georgi A, Kopinke F-D (2005) Interaction of adsorption and catalytic reactions in water decontamination processes: part I. oxidation of organic contaminants with hydrogen peroxide catalyzed by activated carbon. *Appl Catal B Environ* 58:9–18
- Gerken JB, McAlpin JG, Chen JY, Rigsby ML, Casey WH, Britt RD, Stahl SS (2011) Electrochemical water oxidation with cobalt-based electrocatalysts from pH 0–14: the thermodynamic basis for catalyst structure, stability, and activity. *J Am Chem Soc* 133:14431–14442
- Ghaffar A, Younis MN (2014) Adsorption of organic chemicals on graphene coated biochars and its environmental implications. *Green Process Synth* 3:479–487
- Grebel JE, Pignatello JJ, Mitch WA (2010) Effect of halide ions and carbonates on organic contaminant degradation by hydroxyl radical-based advanced oxidation processes in saline waters. *Environ Sci Technol* 44:6822
- Greluk M, Hubicki Z (2010) Kinetics, isotherm and thermodynamic studies of Reactive Black 5 removal by acid acrylic resins. *Chem Eng J* 162:919–926
- Grover D, Zhou J, Frickers P, Readman J (2011) Improved removal of estrogenic and pharmaceutical compounds in sewage effluent by full scale granular activated carbon: impact on receiving river water. *J Hazard Mater* 185:1005–1011
- Guan Y-H, Ma J, Ren Y-M, Liu Y-L, Xiao J-Y, Lin L-q, Zhang C (2013) Efficient degradation of atrazine by magnetic porous copper ferrite catalyzed peroxydisulfate oxidation via the formation of hydroxyl and sulfate radicals. *Water Res* 47:5431–5438
- Guan XJ, Zhou J, Ma N, Chen XY, Gao JQ, Zhang RQ (2015) Studies on modified conditions of biochar and the mechanism for fluoride removal. *Desalin Water Treat* 55:440–447. <https://doi.org/10.1080/19443994.2014.916230>
- Hamid SBA, Chowdhury ZZ, Zain SM (2014) Base catalytic approach: a promising technique for the activation of biochar for equilibrium sorption studies of copper, Cu (II) ions in single solute system. *Materials* 7:2815–2832
- Han D, Liu X, Zhang G, Sun K, Jiao Y (2013) Effects of cationic surfactant on pentachlorophenol sorption by sediment, active carbon and biochar. *Fresenius Environ Bull* 22:1280–1286
- Han L, Xue S, Zhao S, Yan J, Qian L, Chen M (2015a) Biochar supported nanoscale iron particles for the efficient removal of methyl orange dye in aqueous solutions. *PLoS One* 10:e0132067
- Han XY et al (2015b) Removal of methylene blue from aqueous solution using porous biochar obtained by KOH activation of peanut shell biochar. *Bioresources* 10:2836–2849. <https://doi.org/10.15376/biores.10.2.2836-2849>
- Hazime R, Nguyen Q, Ferronato C, Salvador A, Jaber F, Chovelon J-M (2014) Comparative study of imazalil degradation in three systems: UV/TiO<sub>2</sub>, UV/K<sub>2</sub>S<sub>2</sub>O<sub>8</sub> and UV/TiO<sub>2</sub>/K<sub>2</sub>S<sub>2</sub>O<sub>8</sub>. *Appl Catal B Environ* 144:286–291
- Hu WR, Xie Y, Lu S, Li PY, Xie TH, Zhang YK, Wang YB (2019) One-step synthesis of nitrogen-doped sludge carbon as a bifunctional material for the adsorption and catalytic oxidation of organic pollutants. *Sci Total Environ* 680:51. <https://doi.org/10.1016/j.scitotenv.2019.05.098>
- Huang B-C, Jiang J, Huang G-X, Yu H-Q (2018) Sludge biochar-based catalysts for improved pollutant degradation by activating peroxy-monosulfate. *J Mater Chem A* 6:8978–8985. <https://doi.org/10.1039/C8TA02282H>
- Huff MD, Lee JW (2016) Biochar-surface oxygenation with hydrogen peroxide. *J Environ Manag* 165:17–21. <https://doi.org/10.1016/j.jenvman.2015.08.046>
- Hussain I et al (2017) Insights into the mechanism of persulfate activation with nZVI/BC nanocomposite for the degradation of nonylphenol. *Chem Eng J* 311:163–172
- Hutchings GS (2015) Advanced nanostructured materials for energy storage and conversion. University of Delaware, PhD diss
- Inyang M, Dickenson E (2015) The potential role of biochar in the removal of organic and microbial contaminants from potable and reuse water: a review. *Chemosphere* 134:232
- Inyang M, Gao B, Zimmerman A, Zhang M, Chen H (2014) Synthesis, characterization, and dye sorption ability of carbon nanotube-biochar nanocomposites. *Chem Eng J* 236:39–46
- Inyang M, Gao B, Zimmerman A, Zhou Y, Cao X (2015) Sorption and cosorption of lead and sulfapyridine on carbon nanotube-modified biochars. *Environ Sci Pollut Res* 22:1868–1876
- Jafari AJ, Kakavandi B, Jaafarzadeh N, Kalantary RR, Ahmadi M, Babaei AA (2017) Fenton-like catalytic oxidation of tetracycline by AC@ Fe<sub>3</sub>O<sub>4</sub> as a heterogeneous persulfate activator: adsorption and degradation studies. *J Ind Eng Chem* 45:323–333
- Jeon P, Lee M-E, Baik K (2017a) Adsorption and photocatalytic activity of biochar with graphitic carbon nitride (g-C<sub>3</sub>N<sub>4</sub>). *J Taiwan Inst Chem Eng* 77:244–249
- Jeon P, Lee ME, Baik K (2017b) Adsorption and photocatalytic activity of biochar with graphitic carbon nitride (g-C<sub>3</sub>N<sub>4</sub>). *J Taiwan Inst Chem Eng* 77:244–249
- Jiang M, Lu J, Ji Y, Kong D (2017) Bicarbonate-activated persulfate oxidation of acetaminophen. *Water Res* 116:324–331
- Jing X-R, Wang Y-Y, Liu W-J, Wang Y-K, Jiang H (2014) Enhanced adsorption performance of tetracycline in aqueous solutions by methanol-modified biochar. *Chem Eng J* 248:168–174
- Jung C et al (2013) Adsorption of selected endocrine disrupting compounds and pharmaceuticals on activated biochars. *J Hazard Mater* 263:702–710. <https://doi.org/10.1016/j.jhazmat.2013.10.033>
- Jung C, Boateng LK, Flora JRV, Oh J, Braswell MC, Son A, Yoon Y (2015) Competitive adsorption of selected non-steroidal anti-inflammatory drugs on activated biochars: experimental and molecular modeling study. *Chem Eng J* 264:1–9
- Keams JP, Shimabuku KK, Mahoney RB, Knappe DRU, Summers RS (2015) Meeting multiple water quality objectives through treatment using locally generated char: improving organoleptic properties and removing synthetic organic contaminants and disinfection by-products. *J Water Sanit Hyg De* 5:359–372. <https://doi.org/10.2166/washdev.2015.172>
- Keen OS, McKay G, Mezyk SP, Linden KG, Rosario-Ortiz FL (2014) Identifying the factors that influence the reactivity of effluent organic matter with hydroxyl radicals. *Water Res* 50:408–419
- Keiluweit M, Nico PS, Johnson MG, Kleber M (2010) Dynamic molecular structure of plant biomass-derived black carbon (biochar). *Environ Sci Technol* 44:1247–1253
- Kemmou L, Frontistis Z, Vakros J, Manariotis ID, Mantzavinos D (2018) Degradation of antibiotic sulfamethoxazole by biochar-activated persulfate: factors affecting the activation and degradation processes. *Catal Today* 313:128–133

- Khataee A, Kayan B, Gholami P, Kalderis D, Akay S (2017) Sonocatalytic degradation of an anthraquinone dye using TiO<sub>2</sub>-biochar nanocomposite. *Ultrason Sonochem* 39:120–128
- Khataee A, Gholami P, Kalderis D, Pachatouridou E, Konsolakis M (2018) Preparation of novel CeO<sub>2</sub>-biochar nanocomposite for sonocatalytic degradation of a textile dye. *Ultrason Sonochem* 41: 503–513
- Kim D, Park S, Park KY (2017) Upgrading the fuel properties of sludge and low rank coal mixed fuel through hydrothermal carbonization. *Energy* 141:598–602
- Kim J, Park B, Son Y, Khim J (2018) Peat moss-derived biochar for sonocatalytic applications. *Ultrason Sonochem* 42:26–30. <https://doi.org/10.1016/j.ultsonch.2017.11.005>
- Kirisits MJ, Snoeyink VL, Kruihof JC (2000) The reduction of bromate by granular activated carbon. *Water Res* 34:4250–4260
- Klöpffel L, Keilueit M, Kleber M, Sander M (2014) Redox properties of plant biomass-derived black carbon (biochar). *Environ Sci Technol* 48:5601–5611
- Kong L et al (2014) Sorption performance and mechanism of a sludge-derived char as porous carbon-based hybrid adsorbent for benzene derivatives in aqueous solution. *J Hazard Mater* 274:205–211
- Kunde GB, Yadav GD (2015) Synthesis, characterization and application of iron-aluminate nodules in advanced Fenton's oxidation process. *J Environ Chem Eng* 3:2010–2021
- Lan H, Wang A, Liu R, Liu H, Qu J (2015) Heterogeneous photo-Fenton degradation of acid red B over Fe<sub>2</sub>O<sub>3</sub> supported on activated carbon fiber. *J Hazard Mater* 285:167–172
- Lee Y-C, Lo S-L, Chiueh P-T, Chang D-G (2009) Efficient decomposition of perfluorocarboxylic acids in aqueous solution using microwave-induced persulfate. *Water Res* 43:2811–2816
- Lee Y-C, Lo S-L, Kuo J, Huang C-P (2013) Promoted degradation of perfluorooctanoic acid by persulfate when adding activated carbon. *J Hazard Mater* 261:463–469
- Li J, Li Y, Wu Y, Zheng M (2014a) A comparison of biochars from lignin, cellulose and wood as the sorbent to an aromatic pollutant. *J Hazard Mater* 280:450–457
- Li J, Lv G, Bai W, Liu Q, Zhang Y, Song J (2014b) Modification and use of biochar from wheat straw (*Triticum aestivum* L.) for nitrate and phosphate removal from water. *Desalin Water Treat* 57:1–13. <https://doi.org/10.1080/19443994.2014.994104>
- Li Y, Shao J, Wang X, Deng Y, Yang H, Chen H (2014c) Characterization of modified biochars derived from bamboo pyrolysis and their utilization for target component (furfural) adsorption. *Energy Fuel* 28: 5119–5127. <https://doi.org/10.1021/ef500725c>
- Li Z, Chen Z, Xiang Y, Ling L, Fang J, Shang C, Dionysiou DD (2015) Bromate formation in bromide-containing water through the cobalt-mediated activation of peroxymonosulfate. *Water Res* 83:132–140
- Li A, Lin RJ, Lin C, He BY, Zheng TT, Lu LB, Cao Y (2016) An environment-friendly and multi-functional adsorbent from chitosan for organic pollutants and heavy metal ion. *Carbohydr Polym* 148: 272–280. <https://doi.org/10.1016/j.carbpol.2016.04.070>
- Liang CJ, Bruell CJ, Marley MC, Sperry KL (2003) Thermally activated persulfate oxidation of trichloroethylene (TCE) and 1, 1, 1-trichloroethane (TCA) in aqueous systems and soil slurries. *Soil Sediment Contam Int J* 12:207–228
- Liang C, Wang ZS, Mohanty N (2006) Influences of carbonate and chloride ions on persulfate oxidation of trichloroethylene at 20 degrees C. *Sci Total Environ* 370:271–277
- Liang C, Wang Z-S, Bruell CJ (2007) Influence of pH on persulfate oxidation of TCE at ambient temperatures. *Chemosphere* 66: 106–113
- Liu P, Liu W-J, Jiang H, Chen J-J, Li W-W, Yu H-Q (2012) Modification of bio-char derived from fast pyrolysis of biomass and its application in removal of tetracycline from aqueous solution. *Bioresour Technol* 121:235–240
- Liu K, Lu J, Ji Y (2015) Formation of brominated disinfection by-products and bromate in cobalt catalyzed peroxymonosulfate oxidation of phenol. *Water Res* 84:1–7
- Liu XQ, Chen WJ, Jiang H (2017) Facile synthesis of Ag/Ag<sub>3</sub>PO<sub>4</sub>/AMB composite with improved photocatalytic performance. *Chem Eng J* 308:889–896. <https://doi.org/10.1016/j.cej.2016.09.125>
- Liu Z et al (2018) Functionalizing bottom ash from biomass power plant for removing methylene blue from aqueous solution. *Sci Total Environ* 634:760–768. <https://doi.org/10.1016/j.scitotenv.2018.04.010>
- Lomnicki S, Truong H, Vejerano E, Dellinger B (2008) Copper oxide-based model of persistent free radical formation on combustion-derived particulate matter. *Environ Sci Technol* 42:4982–4988. <https://doi.org/10.1021/es071708h>
- Luo S et al (2017) Mechanistic insight into reactivity of sulfate radical with aromatic contaminants through single-electron transfer pathway. *Chem Eng J* 327:1056–1065. <https://doi.org/10.1016/j.cej.2017.06.179>
- Luo M, Lin H, Li B, Dong Y, He Y, Wang L (2018) A novel modification of lignin on corn-cob-based biochar to enhance removal of cadmium from water. *Bioresour Technol* 259:312–318
- Luo K, Yang Q, Pang Y, Wang D, Li X, Lei M, Huang Q (2019) Unveiling the mechanism of biochar-activated hydrogen peroxide on the degradation of ciprofloxacin. *Chem Eng J* 374:520–530. <https://doi.org/10.1016/j.cej.2019.05.204>
- Mahmoud ME, Nabil GM, El-Mallah NM, Bassiouny HI, Kumar S, Abdel-Fattah TM (2016) Kinetics, isotherm, and thermodynamic studies of the adsorption of reactive red 195 A dye from water by modified Switchgrass Biochar adsorbent. *J Ind Eng Chem* 37: 156–167
- Manyà JJ, Azuara M, Manso JA (2018) Biochar production through slow pyrolysis of different biomass materials: seeking the best operating conditions. *Biomass Bioenergy* 117:115–123. <https://doi.org/10.1016/j.biombioe.2018.07.019>
- Masel RI (1996) Principles of adsorption and reaction on solid surfaces, vol 3. John Wiley & Sons, Canada
- Méndezdiaz J, Sánchezpolo M, Riverautrilla J, Canonica S, Gunten UV (2010) Advanced oxidation of the surfactant SDBS by means of hydroxyl and sulphate radicals. *Chem Eng J* 163:300–306
- Meri NH, Alias AB, Talib N, Rashid ZA, Ghani WAWA (2018) Effect of chemical washing pre-treatment of empty fruit bunch (EFB) biochar on characterization of hydrogel biochar composite as bioadsorbent. Paper presented at the 3rd International Conference on Global Sustainability and Chemical Engineering (Icgsce)
- Mertens R, von Sonntag C (1995) Photolysis ( $\lambda = 354$  nm of tetrachloroethene in aqueous solutions). *J Photochem Photobiol A Chem* 85:1–9
- Mi X, Li G, Zhu W, Liu L (2016) Enhanced adsorption of orange II using cationic surfactant modified biochar pyrolyzed from cornstarch. *J Chemother* 2016:1–7. <https://doi.org/10.1155/2016/8457030>
- Mian MM, Liu G (2018) Recent progress in biochar-supported photocatalysts: synthesis, role of biochar, and applications. *RSC Adv* 8:14237–14248
- Muhammad S, Shukla PR, Tadé MO, Wang S (2012) Heterogeneous activation of peroxymonosulphate by supported ruthenium catalysts for phenol degradation in water. *J Hazard Mater* 215:183–190
- Nawi M, Jawad AH, Sabar S, Ngah WW (2011) Immobilized bilayer TiO<sub>2</sub>/chitosan system for the removal of phenol under irradiation by a 45 watt compact fluorescent lamp. *Desalination* 280:288–296
- Neta P, Madhavan V, Zemel H, Fessenden RW (1977) Rate constants and mechanism of reaction of sulfate radical anion with aromatic compounds. *J Am Chem Soc* 99:163–164
- Novak J, Ro K, Ok YS, Sigua G, Spokas K, Uchimiya S, Bolan N (2016) Biochars multifunctional role as a novel technology in the agricultural, environmental, and industrial sectors. *Chemosphere* 142:1–3



- Ok YS, Chang SX, Gao B, Chung HJ (2015) SMART biochar technology—a shifting paradigm towards advanced materials and healthcare research. *Environ Technol Innov* 4:206–209. <https://doi.org/10.1016/j.eti.2015.08.003>
- Okay O (2009) General properties of hydrogels. In: *Hydrogel sensors and actuators*. Springer Series on Chemical Sensors and Biosensors. Springer, Berlin, pp 1–14. [https://doi.org/10.1007/978-3-540-75645-3\\_1](https://doi.org/10.1007/978-3-540-75645-3_1)
- Oladipo AA, Ifebajo AO (2017) Highly efficient magnetic chicken bone biochar for removal of tetracycline and fluorescent dye from wastewater: two-stage adsorber analysis. *J Environ Manag* 209:9–16
- Ouyang D et al (2017) Degradation of 1, 4-dioxane by biochar supported nano magnetite particles activating persulfate. *Chemosphere* 184: 609–617
- Paria S (2008) Surfactant-enhanced remediation of organic contaminated soil and water. *Adv Colloid Interf Sci* 138:24–58
- Park JH, Wang JJ, Xiao R, Tafti N, DeLaune RD, Seo DC (2018) Degradation of orange G by Fenton-like reaction with Fe-impregnated biochar catalyst. *Bioresour Technol* 249:368–376. <https://doi.org/10.1016/j.biortech.2017.10.030>
- Peng X et al (2017) New insights into the activity of a biochar supported nanoscale zerovalent iron composite and nanoscale zero valent iron under anaerobic or aerobic conditions. *RSC Adv* 7: 8755–8761
- Pi L, Jiang R, Zhou W, Zhu H, Xiao W, Wang D, Mao X (2015) g-C<sub>3</sub>N<sub>4</sub> modified biochar as an adsorptive and photocatalytic material for decontamination of aqueous organic pollutants. *Appl Surf Sci* 358: 231–239
- Pi ZJ et al (2019) Persulfate activation by oxidation biochar supported magnetite particles for tetracycline removal: performance and degradation pathway. *J Clean Prod* 235:1103–1115. <https://doi.org/10.1016/j.jclepro.2019.07.037>
- Prieto-Rodríguez L, Oller I, Klammerth N, Agüera A, Rodríguez E, Malato S (2013) Application of solar AOPs and ozonation for elimination of micropollutants in municipal wastewater treatment plant effluents. *Water Res* 47:1521–1528
- Qin J, Chen Q, Sun M, Sun P, Shen G (2017) Pyrolysis temperature-induced changes in the catalytic characteristics of rice husk-derived biochar during 1, 3-dichloropropene degradation. *Chem Eng J* 330:804–812
- Rajapaksha AU et al (2016) Engineered/designer biochar for contaminant removal/immobilization from soil and water: potential and implication of biochar modification. *Chemosphere* 148:276–291. <https://doi.org/10.1016/j.chemosphere.2016.01.043>
- Rastogi A, Al-Abed SR, Dionysiou DD (2009a) Effect of inorganic, synthetic and naturally occurring chelating agents on Fe(II) mediated advanced oxidation of chlorophenols. *Water Res* 43:684–694
- Rastogi A, Al-Abed SR, Dionysiou DD (2009b) Sulfate radical-based ferrous–peroxymonosulfate oxidative system for PCBs degradation in aqueous and sediment systems. *Appl Catal B Environ* 85: 171–179
- Regmi P, Moscoso JLG, Kumar S, Cao X, Mao J, Schafran G (2012) Removal of copper and cadmium from aqueous solution using switchgrass biochar produced via hydrothermal carbonization process. *J Environ Manag* 109:61–69
- Saleh MM (2006) On the removal of cationic surfactants from dilute streams by granular charcoal. *Water Res* 40:1052–1060
- Santhanalakshmi J, Balaji S (1996) Adsorption studies of nonionic surfactants on charcoal and alumina in aromatic solvents. *J Colloid Interface Sci* 179:517–521
- Setianingsih T, Masruri M, Ismuyanto B (2018) Synthesis of patchouli biochar Cr<sub>2</sub>O<sub>3</sub> composite using double acid oxidators for paracetamol adsorption. *J Pure App Chem Res* 7:60–69
- Shen W, Li Z, Liu Y (2008) Surface chemical functional groups modification of porous carbon. *Recent Patents Chem Eng* 1:27–40
- Shen B, Li G, Wang F, Wang Y, He C, Zhang M, Singh S (2015) Elemental mercury removal by the modified bio-char from medicinal residues. *Chem Eng J* 272:28–37
- Snyder SA et al (2007) Role of membranes and activated carbon in the removal of endocrine disruptors and pharmaceuticals. *Desalination* 202:156–181
- Song R, Bai B, Puma GL, Wang H, Suo Y (2015) Biosorption of azo dyes by raspberry-like Fe<sub>3</sub>O<sub>4</sub>@ yeast magnetic microspheres and their efficient regeneration using heterogeneous Fenton-like catalytic processes over an up-flow packed reactor. *React Kinet Mech Catal* 115: 547–562
- Sun L, Chen D, Wan S, Yu Z (2015) Performance, kinetics, and equilibrium of methylene blue adsorption on biochar derived from eucalyptus saw dust modified with citric, tartaric, and acetic acids. *Bioresour Technol* 198:300–308
- Sun H, Peng X, Zhang S, Liu S, Xiong Y, Tian S, Fang J (2017) Activation of peroxymonosulfate by nitrogen-functionalized sludge carbon for efficient degradation of organic pollutants in water. *Bioresour Technol* 241:244–251
- Tan X, Liu Y, Zeng G, Wang X, Hu X, Gu Y, Yang Z (2015) Application of biochar for the removal of pollutants from aqueous solutions. *Chemosphere* 125:70–85
- Tan XF et al (2016) Biochar-based nano-composites for the decontamination of wastewater: a review. *Bioresour Technol* 212:318–333. <https://doi.org/10.1016/j.biortech.2016.04.093>
- Tang L et al (2017) Treatment of arsenic in acid wastewater and river sediment by Fe@ Fe<sub>2</sub>O<sub>3</sub> nanobunches: the effect of environmental conditions and reaction mechanism. *Water Res* 117:175–186
- Tang L et al (2018) Sustainable efficient adsorbent: alkali-acid modified magnetic biochar derived from sewage sludge for aqueous organic contaminant removal. *Chem Eng J* 336:160–169. <https://doi.org/10.1016/j.cej.2017.11.048>
- Toor R, Mohseni M (2007) UV-H<sub>2</sub>O<sub>2</sub> based AOP and its integration with biological activated carbon treatment for DBP reduction in drinking water. *Chemosphere* 66:2087–2095
- Tully F, Ravishankara A, Thompson R, Nicovich J, Shah R, Kreutter N, Wine P (1981) Kinetics of the reactions of hydroxyl radical with benzene and toluene. *J Phys Chem* 85:2262–2269
- Uchimiya M, Lima IM, Klasson KT, Wartelle LH (2010) Contaminant immobilization and nutrient release by biochar soil amendment: roles of natural organic matter. *Chemosphere* 80:935–940
- Usman M, Faure P, Ruby C, Hanna K (2012) Application of magnetite-activated persulfate oxidation for the degradation of PAHs in contaminated soils. *Chemosphere* 87:234–240
- Vejerano E, Lomnicki S, Dellinger B (2010) Formation and stabilization of combustion-generated environmentally persistent free radicals on an Fe (III)O<sub>3</sub>/silica surface. *Environ Sci Technol* 45:589–594. <https://doi.org/10.1021/es102841s>
- Von Sonntag C, Von Gunten U (2012) *Chemistry of ozone in water and wastewater treatment*. IWA publishing, London
- Wang GS, Hsieh ST, Hong CS (2000) Destruction of humic acid in water by UV light—catalyzed oxidation with hydrogen peroxide. *Water Res* 34:3882–3887
- Wang Z, Yuan R, Guo Y, Xu L, Liu J (2011) Effects of chloride ions on bleaching of azo dyes by Co<sup>2+</sup>/oxone reagent: kinetic analysis. *J Hazard Mater* 190:1083–1087
- Wang Y, Le Roux J, Zhang T, Croué J-P (2014) Formation of brominated disinfection byproducts from natural organic matter isolates and model compounds in a sulfate radical-based oxidation process. *Environ Sci Technol* 48:14534–14542
- Wang B, Lehmann J, Hanley K, Hestrin R, Enders A (2015) Adsorption and desorption of ammonium by maple wood biochar as a function of oxidation and pH. *Chemosphere* 138:120–126

- Wang B, Lehmann J, Hanley K, Hestrin R, Enders A (2016a) Ammonium retention by oxidized biochars produced at different pyrolysis temperatures and residence times. *RSC Adv* 6:41907–41913
- Wang Q et al (2016b) Degradation kinetics and mechanism of 2,4-di-tert-butylphenol with UV/persulfate. *Chem Eng J* 304:201–208. <https://doi.org/10.1016/j.cej.2016.06.092>
- Wang Y, Ao Z, Sun H, Duan X, Wang S (2016c) Activation of peroxy-monosulfate by carbonaceous oxygen groups: experimental and density functional theory calculations. *Appl Catal B Environ* 198: 295–302
- Wang G, Chen S, Quan X, Yu H, Zhang Y (2017a) Enhanced activation of peroxy-monosulfate by nitrogen doped porous carbon for effective removal of organic pollutants. *Carbon* 115:730–739
- Wang J et al (2017b) Treatment of refractory contaminants by sludge-derived biochar/persulfate system via both adsorption and advanced oxidation process. *Chemosphere* 185:754–763. <https://doi.org/10.1016/j.chemosphere.2017.07.084>
- Wang HZ et al (2019) Edge-nitrogenated biochar for efficient peroxydisulfate activation: an electron transfer mechanism. *Water Res* 160:405–414. <https://doi.org/10.1016/j.watres.2019.05.059>
- Wu Y, Guo J, Han Y, Zhu J, Zhou L, Lan Y (2018) Insights into the mechanism of persulfate activated by rice straw biochar for the degradation of aniline. *Chemosphere* 200:373–379
- Xia D et al (2016) ZnCl<sub>2</sub>-activated biochar from biogas residue facilitates aqueous As(III) removal. *Appl Surf Sci* 377:361–369
- Xiao R, Ye T, Wei Z, Luo S, Yang Z, Spinney R (2015) Quantitative structure–activity relationship (QSAR) for the oxidation of trace organic contaminants by sulfate radical. *Environ Sci Technol* 49: 13394–13402
- Xie M, Chen W, Xu Z, Zheng S, Zhu D (2014) Adsorption of sulfonamides to demineralized pine wood biochars prepared under different thermochemical conditions. *Environ Pollut* 186:187–194. <https://doi.org/10.1016/j.envpol.2013.11.022>
- Xu X, Zhao Y, Sima J, Zhao L, Mašek O, Cao X (2017) Indispensable role of biochar-inherent mineral constituents in its environmental applications: a review. *Bioresour Technol* 241:887–899
- Xue Y, Gao B, Yao Y, Inyang M, Zhang M, Zimmerman AR, Ro KS (2012) Hydrogen peroxide modification enhances the ability of biochar (hydrochar) produced from hydrothermal carbonization of peanut hull to remove aqueous heavy metals: batch and column tests. *Chem Eng J* 200:673–680
- Yakout SM (2015) Monitoring the changes of chemical properties of rice straw-derived biochars modified by different oxidizing agents and their adsorptive performance for organics. *Bioremediat J* 19: 171–182
- Yan L, Kong L, Qu Z, Li L, Shen G (2014) Magnetic biochar decorated with ZnS nanocrystals for Pb(II) removal. *ACS Sustain Chem Eng* 3: 125–132
- Yan J, Han L, Gao W, Xue S, Chen M (2015) Biochar supported nanoscale zerovalent iron composite used as persulfate activator for removing trichloroethylene. *Bioresour Technol* 175:269–274
- Yan J, Qian L, Gao W, Chen Y, Ouyang D, Chen M (2017) Enhanced Fenton-like degradation of trichloroethylene by hydrogen peroxide activated with nanoscale zero valent iron loaded on biochar. *Sci Rep* 7:43051
- Yang G-X, Jiang H (2014) Amino modification of biochar for enhanced adsorption of copper ions from synthetic wastewater. *Water Res* 48: 396–405
- Yang S, Yang X, Shao X, Niu R, Wang L (2011) Activated carbon catalyzed persulfate oxidation of azo dye acid orange 7 at ambient temperature. *J Hazard Mater* 186:659–666
- Yang G, Chen H, Qin H, Feng Y (2014) Amination of activated carbon for enhancing phenol adsorption: effect of nitrogen-containing functional groups. *Appl Surf Sci* 293:299–305
- Yang J, Pan B, Li H, Liao S, Zhang D, Wu M, Xing B (2015) Degradation of p-nitrophenol on biochars: role of persistent free radicals. *Environ Sci Technol* 50:694–700
- Yao Y, Gao B, Chen J, Yang L (2013) Engineered biochar reclaiming phosphate from aqueous solutions: mechanisms and potential application as a slow-release fertilizer. *Environ Sci Technol* 47: 8700–8708
- Yao Y et al (2014) Characterization and environmental applications of clay–biochar composites. *Chem Eng J* 242:136–143
- Yen CH, Chen KF, Kao CM, Liang SH, Chen TY (2011) Application of persulfate to remediate petroleum hydrocarbon-contaminated soil: feasibility and comparison with common oxidants. *J Hazard Mater* 186:2097–2102. <https://doi.org/10.1016/j.jhazmat.2010.12.129>
- Yu W, Lian F, Cui G, Liu Z (2018) N-doping effectively enhances the adsorption capacity of biochar for heavy metal ions from aqueous solution. *Chemosphere* 193:8–16
- Yu J et al (2019a) Magnetic nitrogen-doped sludge-derived biochar catalysts for persulfate activation: Internal electron transfer mechanism. *Chem Eng J* 364:146–159
- Yu JF et al (2019b) Hierarchical porous biochar from shrimp shell for persulfate activation: a two-electron transfer path and key impact factors. *Appl Catal B Environ* 260. <https://doi.org/10.1016/j.apcatb.2019.118160>
- Zazo J, Casas J, Mohedano A, Rodríguez J (2006) Catalytic wet peroxide oxidation of phenol with a Fe/active carbon catalyst. *Appl Catal B Environ* 65:261–268
- Zeng T, Zhang X, Wang S, Niu H, Cai Y (2014) Spatial confinement of Co<sub>3</sub>O<sub>4</sub> catalyst in hollow metal–organic framework as nanoreactor for improved degradation of organic pollutant. *Environ Sci Technol* 49:2350
- Zhang M, Gao B, Yao Y, Xue Y, Inyang M (2012) Synthesis, characterization, and environmental implications of graphene-coated biochar. *Sci Total Environ* 435–436:567–572
- Zhang XN, Mao GY, Jiao YB, Shang Y, Han RP (2014) Adsorption of anionic dye on magnesium hydroxide-coated pyrolytic bio-char and reuse by microwave irradiation. *Int J Environ Sci Technol (Tehran)* 11:1439–1448
- Zhang B-T, Zhang Y, Teng Y, Fan M (2015) Sulfate radical and its application in decontamination technologies. *Crit Rev Environ Sci Technol* 45:1756–1800
- Zhang Y, Liu C, Xu B, Qi F, Chu W (2016) Degradation of benzotriazole by a novel Fenton-like reaction with mesoporous Cu/MnO<sub>2</sub>: combination of adsorption and catalysis oxidation. *Appl Catal B Environ* 199:447–457
- Zhang H, Wang Z, Li R, Guo J, Li Y, Zhu J, Xie X (2017) TiO<sub>2</sub> supported on reed straw biochar as an adsorptive and photocatalytic composite for the efficient degradation of sulfamethoxazole in aqueous matrices. *Chemosphere* 185:351–360
- Zhang K, Sun P, Faye MCAS, Zhang Y (2018a) Characterization of biochar derived from rice husks and its potential in chlorobenzene degradation. *Carbon* 130:730–740
- Zhang Y, Cao B, Zhao L, Sun L, Gao Y, Li J, Yang F (2018b) Biochar-supported reduced graphene oxide composite for adsorption and coadsorption of atrazine and lead ions. *Appl Surf Sci* 427:147–155
- Zhang C, Zhang N, Xiao Z, Li Z, Zhang D (2019a) Characterization of biochars derived from different materials and their effects on microbial dechlorination of pentachlorophenol in a consortium. *RSC Adv* 9:917–923. <https://doi.org/10.1039/C8RA09410A>

- Zhang P et al (2019b) Catalytic degradation of estrogen by persulfate activated with iron-doped graphitic biochar: process variables effects and matrix effects. *Chem Eng J*:378. <https://doi.org/10.1016/j.cej.2019.122141>
- Zhou J, Zhang Z, Banks E, Grover D, Jiang J (2009) Pharmaceutical residues in wastewater treatment works effluents and their impact on receiving river water. *J Hazard Mater* 166:655–661
- Zhou Y, Gao B, Zimmerman AR, Fang J, Sun Y, Cao X (2013) Sorption of heavy metals on chitosan-modified biochars and its biological effects. *Chem Eng J* 231:512–518
- Zhou X et al (2019) Persulfate activation by swine bone char-derived hierarchical porous carbon: multiple mechanism system for organic pollutant degradation in aqueous media. *Chem Eng J*: <https://doi.org/10.1016/j.cej.2019.123091>
- Zhu B, Fan T, Zhang D (2008) Adsorption of copper ions from aqueous solution by citric acid modified soybean straw. *J Hazard Mater* 153:300
- Zhu S, Huang X, Ma F, Wang L, Duan X, Wang S (2018) Catalytic removal of aqueous contaminants on n-doped graphitic biochars: inherent roles of adsorption and nonradical mechanisms. *Environ Sci Technol* 52:8649–8658
- Zou Y, Li W, Yang L, Xiao F, An G, Wang Y, Wang D (2019) Activation of peroxymonosulfate by sp<sup>2</sup>-hybridized microalgae-derived carbon for ciprofloxacin degradation: importance of pyrolysis temperature. *Chem Eng J* 370:1286–1297

**Publisher's note** Springer Nature remains neutral with regard to jurisdictional claims in published maps and institutional affiliations.